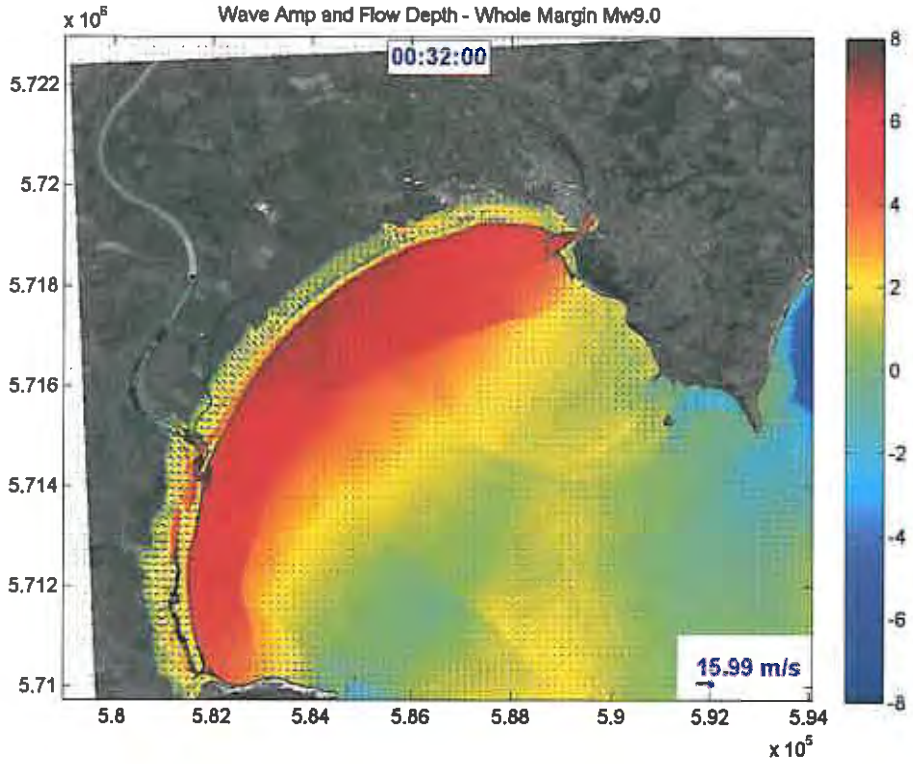

Figure 8.2.5.1-4.c Snapshot of tsunami propagation inside Poverty Bay after the first wave overtops the sand dunes with inundation height above the ground (on land) and the tsunami amplitude (in water). The arrow in the lower right corner shows the scale for the velocity vectors.

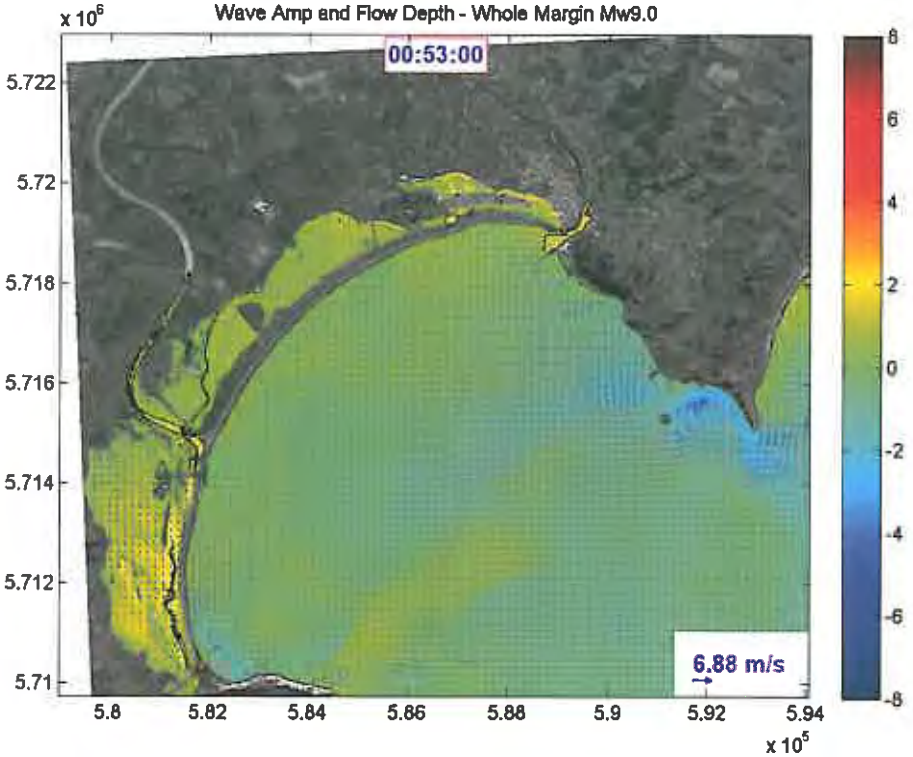

Figure 8.2.5.1-4.d Snapshot of tsunami inundation inside Poverty Bay during the drawdown, where the sand dunes act as a barrier to flows heading back to sea, hence most of the seawater flows back to sea as gravitational flows through low lying areas. The arrow in the lower right corner shows the scale for the velocity vectors.

Gisborne City

With this scenario, the tsunami inundates the coastal areas of Gisborne City directly from the seaside where the waves overtop the sand dunes, and also from the flow that rushes up through the Turanganui River and Waikanae Creek. The maximum inundation and flow depth distribution (Figure 8.2.5.1-5) shows the inundation height distribution along the shoreline is greater than 7.0 m as well as to the eastern part along the cliff. Cliffs are the dominant topographic feature of the eastern part of the bay, from Tuaheni Point down to the port. This causes the maximum flow depth of 11.0 m flowing in a SE-NW direction which occurs along the cliff of Titirangi Domain. The flows surge into the wharf and port, creating a high flow speed of up to 6.0 - 7.0 m/s that over-washes the wharf and port areas, while on the sea side, the flows overtop the breakwater and refract toward the interior of the port basin (Figure 8.2.5.1-5.a and b). These flows are very dangerous to the port facility located at the wharf.

The inundation pattern shows that strong flow speeds are generated in areas where the sand dunes are lowest and also at the access way (Figure 8.2.5.1-5.c and d). These are at Churchill Park and the access way from the beach to Grey Street. Flow speeds of up to 11.0 m/s were generated with flow depths between 2.0 – 4.0 m. Further inland, the leading inundation flow has a speed of 9.0 m/s with flow depth 1.0 m, followed by a higher flow depth of up to 3.0 m with flow speed of 4.0 m/s. While the flow speed in the areas near the port (Customhouse Street and Pitt Street) are relatively low (up to 1 m/s), most of the areas around the port (The Esplanade Road) were inundated. The high flow speeds continue into the Awapuni area with maximum flow speeds of 5.0 m/s. The flow crosses the Waikanae Creek, and bends to the west toward the airport, and follows the stream to the north. The airport area (the runway) is safe.

Most of the flows that overtop the sand dunes in front of the Racecourse (west of Watson Park) are diverted to the west, as the land on Awapuni Road is relatively high. The flow speed when the tsunami overtops the sand dunes reaches ~ 9.0 m/s. There is no return flow to the sea in these areas, as the sand dunes are relatively high, and the inundation flow continues to the west. The areas around the Railyards area are inundated by up to 2.5 m of water. Inundation continues further north across the Waikanae Creek up to Pitt Street, Kahutia Street, Anzac Street, Waitangi Street and Carnarvon Street. The return flows are through Waikanae Creek as the sand dunes along the coast are relatively high. This return flow causes strong currents of up to 2 m/s around the Port areas (Figure 8.2.5.1-5.e and f).

Figure 8.2.5.1-5 Maximum tsunami inundation and flow depth at Gisborne City and surrounding areas (Mean Sea Level, Whole Margin Plate Interface, M_W 9.0).

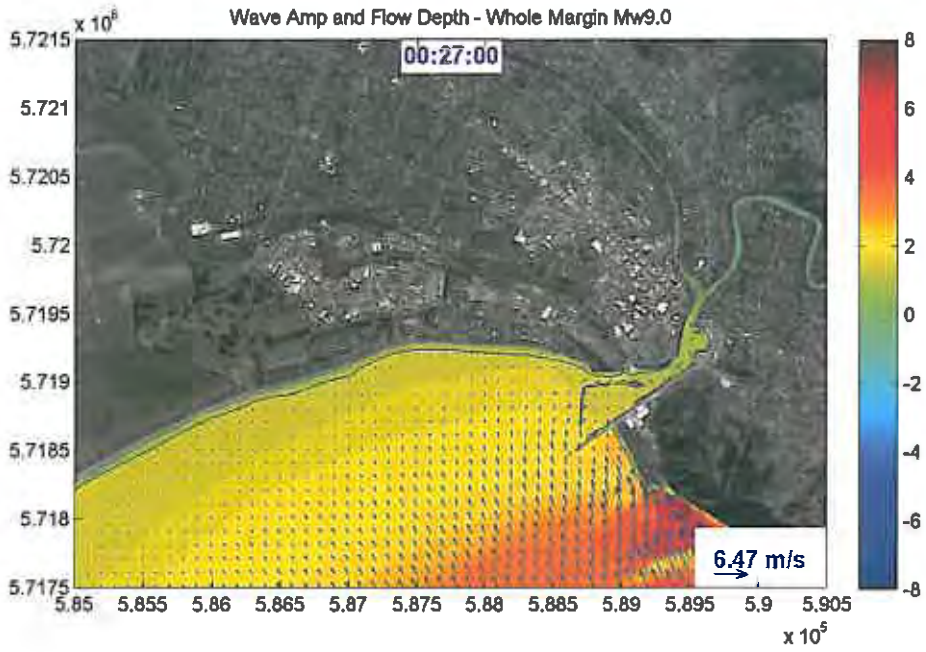

Figure 8.2.5.1-5.a Snapshot of tsunami propagation along the Cliff with high speed flows (~ 6 m/s) towards the Wharf. The arrow in the lower right corner shows the scale for the velocity vectors. The scale bar is in metres.

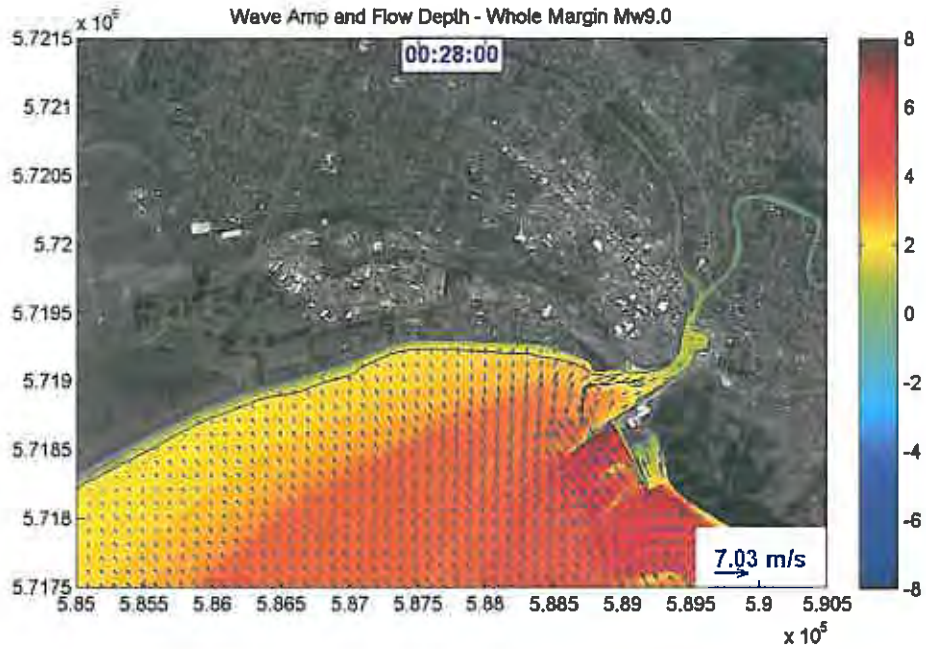

Figure 8.2.5.1-5.b Snapshot of tsunami propagation that over-washes the Wharf where many logs are stored. The arrow in the lower right corner shows the scale for the velocity vectors. The scale bar is in metres.

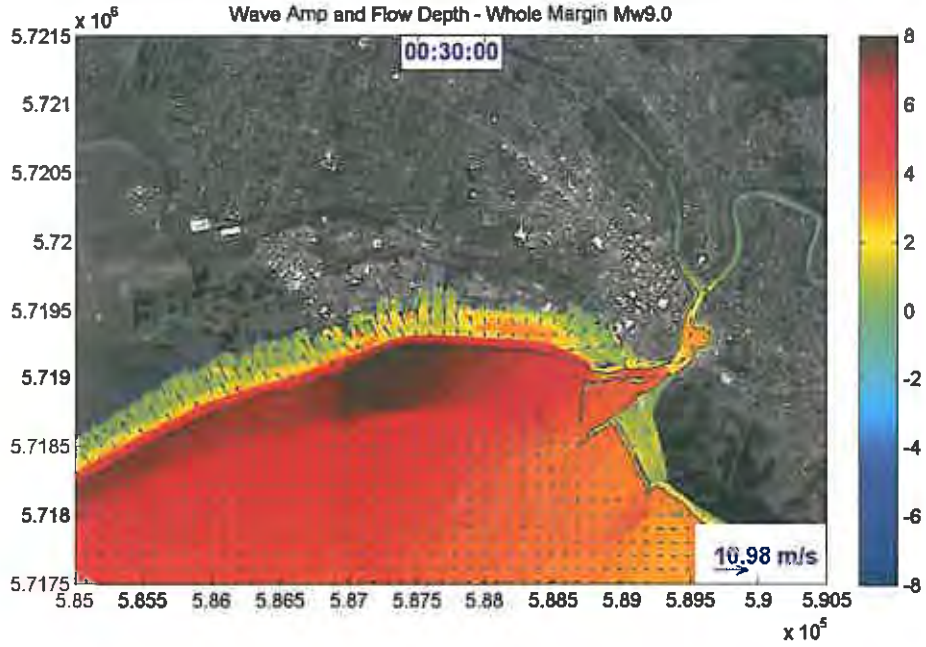

Figure 8.2.5.1-5.c Snapshot of the tsunami propagation that completely over-washes the Wharf and overtops the sand dunes along the coast. The highest flow speed occurs at the sand dune gaps (access way) and the lowest sand dunes areas. The arrow in the lower right corner shows the scale for the velocity vectors. The scale bar is in metres.

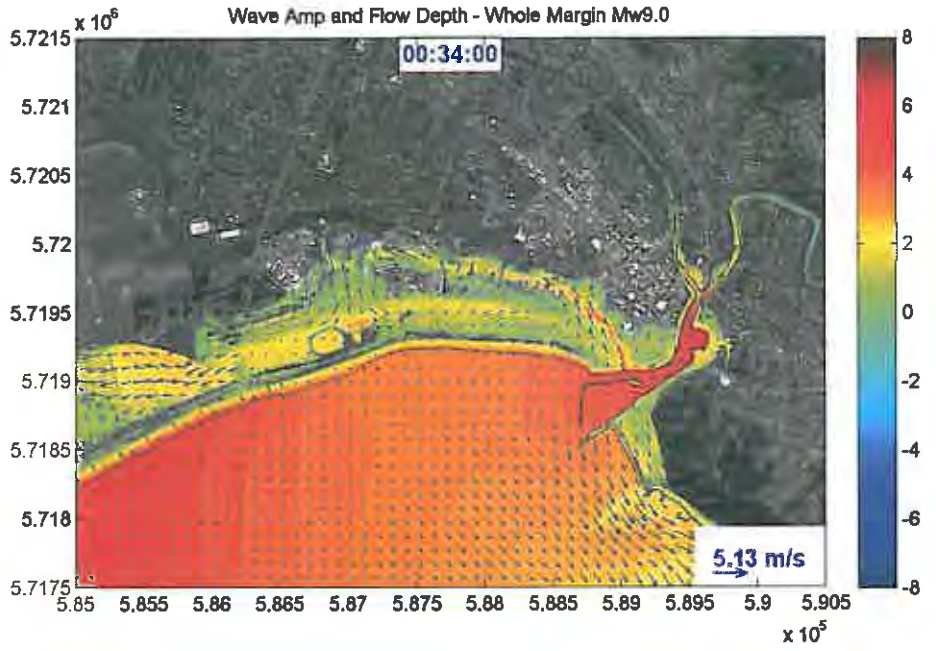

Figure 8.2.5.1-5.d Snapshot of a complex inundation pattern that shows some of the flow has been diverted or converged inland. The arrow in the lower right corner shows the scale for the velocity vectors. The scale bar is in metres.

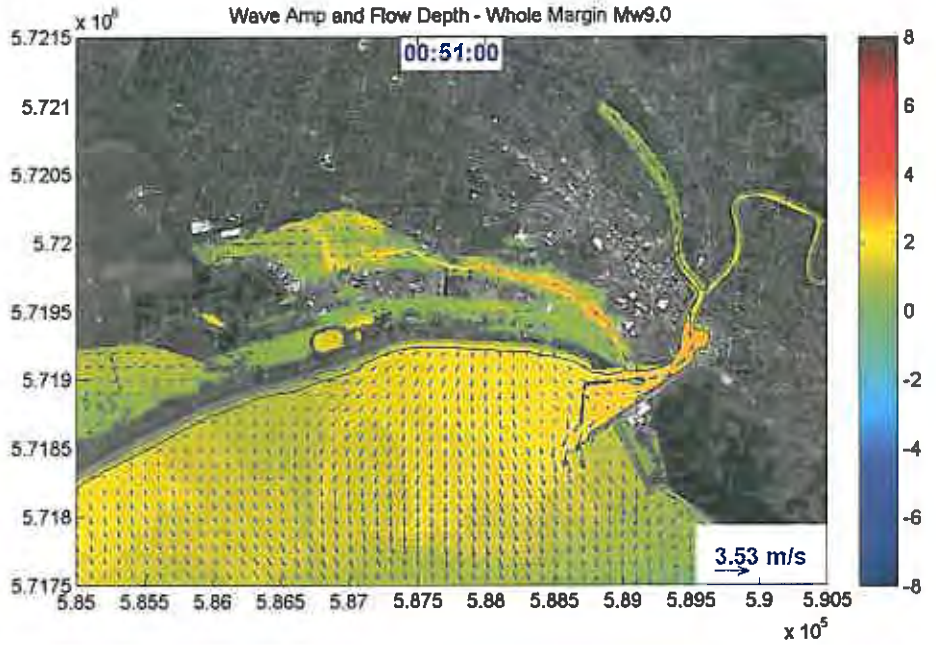

Figure 8.2.5.1.5.e Snapshot of an inundation pattern further inland with some of the seawater retreating through the low-lying areas, Waikanae Creek, and Turanganui River. It is obvious that the sand dunes act as barrier for the flows returning back to the sea. The arrow in the lower right corner shows the scale for the velocity vectors. The scale bar is in metres.

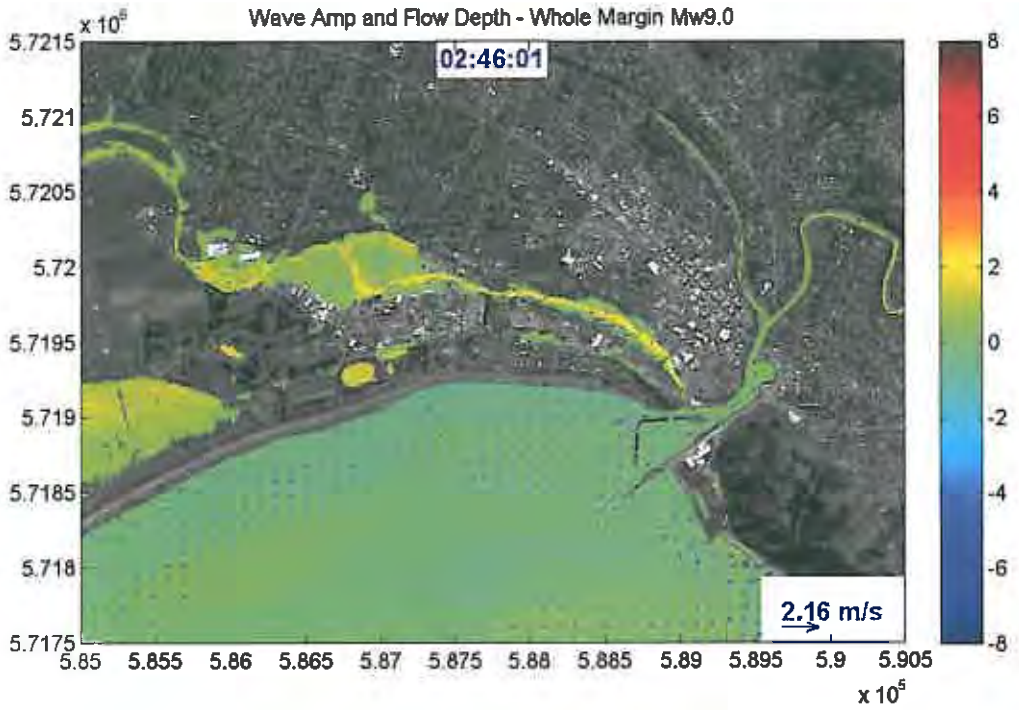

Figure 8.2.5.1.5.f Snapshot of further draining processes through the low-lying areas, Waikanae Creek, and Turanganui River that creates relatively strong currents outside the Port. The arrow in the lower right corner shows the scale for the velocity vectors. The scale bar is in metres.

Wainui

The tsunami inundates the coastal areas of Wainui mostly through the creek as shown in Figure 8.2.5.1-6. Twenty two (22) minutes after the quake, the tsunami with a 4.0 m elevation arrives at the coast (Figure 8.2.5.1-6.a). Within four minutes, the highest elevation of the first waves reaches to greater than 8.0 m, and hits the coastal areas along Wainui Road. However, as the beach faces are very steep with most of the flat areas above the 10.0 m land contour, most of the inundation occurs through the creek. The creek is deep and narrow except at the downstream end, so inundation is not extensive further upstream (Figure 8.2.5.1-6.b). The areas at the end of Wainui Road where there is a bridge over the creek are inundated, and the inundation continues following the local terrain at this site. The return flows at this site are very quick (Figure 8.2.5.1-6.d). Within 20 minutes, most of the seawater has drained back to the sea (Figure 8.2.5.1-6.d). The following tsunami waves with a height of less than 5.0 m did not inundate the coastal areas at this site.

Figure 8.2.5.1-6 Maximum inundation and flow depth at Wainui areas (Mean Sea Level, Whole Margin Plate Interface, M_W 9.0).

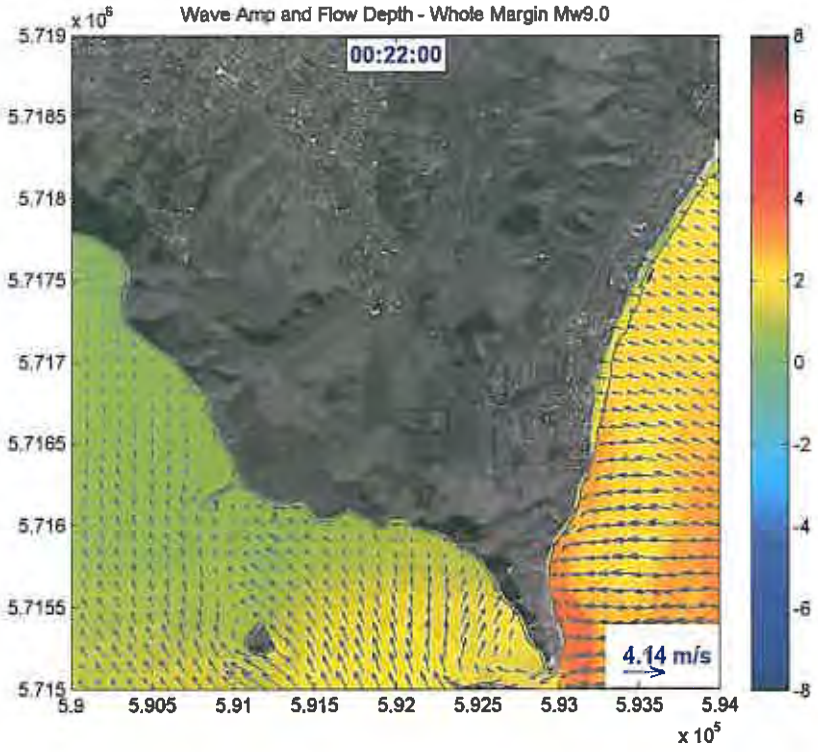

Figure 8.2.5.1-6.a Snapshot of tsunami propagation that starts to inundate the Wainui coastal area. The arrow in the lower right corner shows the scale for the velocity vectors. The scale bar is in metres.

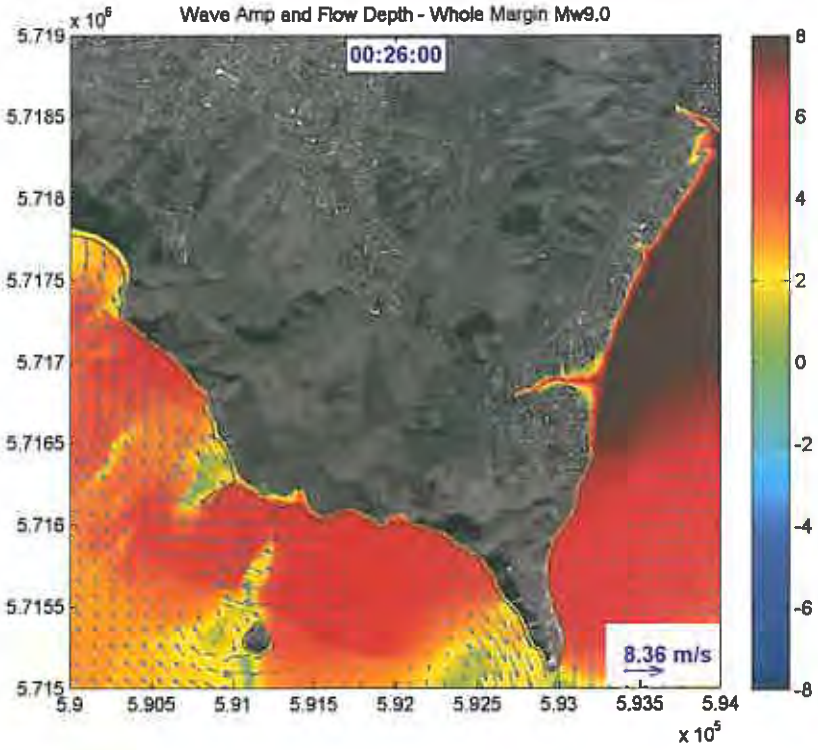

Figure 8.2.5.1-6.b Snapshot of tsunami propagation that inundates the Wainui area mostly through the creeks. Tsunami amplitude along the coast of Wainui is greater than 8 m. The arrow in the lower right corner shows the scale for the velocity vectors. The scale bar is in metres.

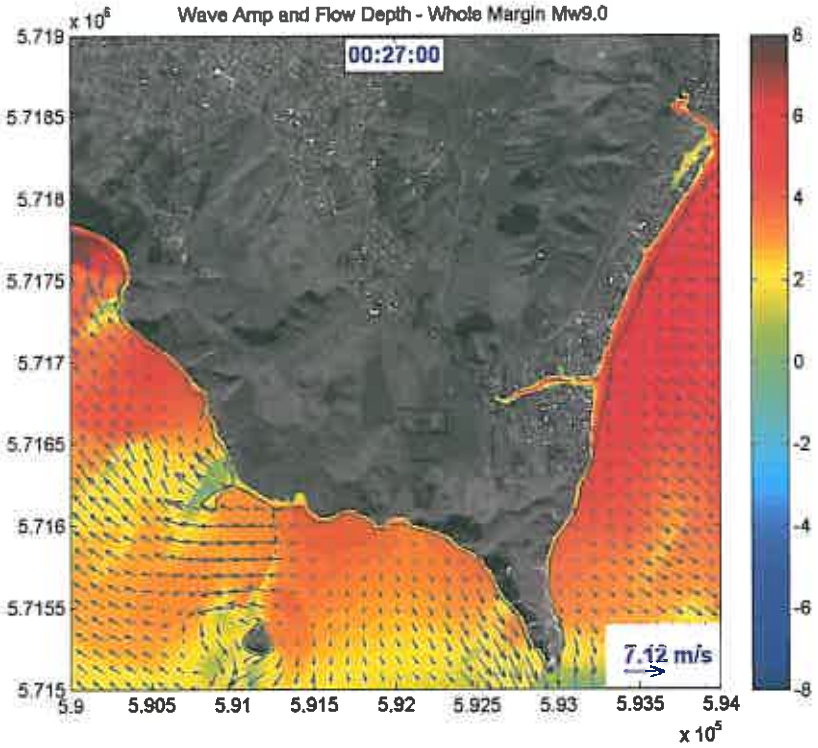

Figure 8.2.5.1-6.c Snapshot of tsunami dynamics during the returning flow from the Wainui coastal area. The arrow in the lower right corner shows the scale for the velocity vectors. The scale bar is in metres.

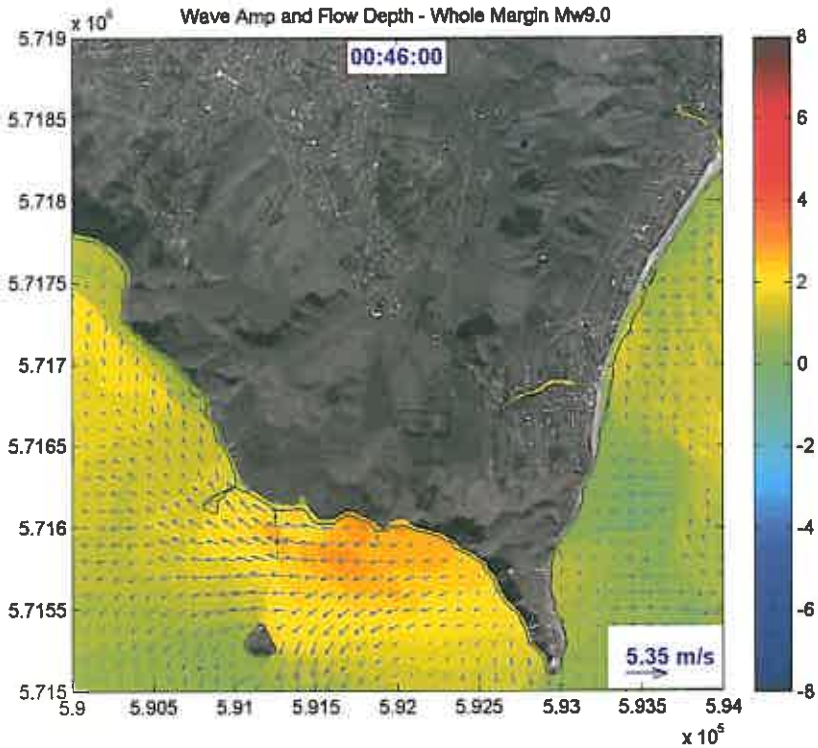

Figure 8.2.5.1-6.d Most of the seawater flows back through the creeks to the sea within ~ 20 minutes of the tsunami reaching its maximum inundation. The arrow in the lower right corner shows the scale for the velocity vectors. The scale bar is in metres.

Muriwai

The Muriwai area at the southwestern end of Poverty Bay up to the Waipaoa River is the most vulnerable area since the local coastal terrain is very flat with a maximum beach face height of 1.0 m above the Mean Sea Level. With this scenario, most of the low-lying areas at Muriwai and the adjacent shore are completely inundated (Figure 8.2.5.1-7). Twenty nine minutes after the earthquake, the leading positive waves with elevation ~ 5.0 m start to overtop the sand spit and inundate Wherowhero lagoon with flow speeds of up to 11.0 m/s (Figure 8.2.5.1-7.a). Within 8 minutes of the tsunami arriving at the coast the flow speed is still high (~10.0 m/s) with flow depth of 2.0 – 4.0 m even though the tsunami has already inundated almost 1.3 km inland (Figure8.2.5.1-7.b). At this stage, the sand dunes to the north of the Waipaoa River are overtopped and the flows inundate the low-lying areas behind the dunes. Complex inundation flow patterns are produced, and the flow speeds at some places are still high ~ 6 m/s and the flow depth is still ~ 2 m at a distance of 1.3 km from the shoreline (Figure 8.2.5.1-7.c). When the inundation reaches Wharerata Road, the flows are diverted to the north, following the local terrain. The maximum inundation of the first waves that reach Wharerata Road is 1.8 km from the shoreline. The second wave that comes an hour later inundates the inlet areas of Wherowhero Lagoon, and extends the inundation further inland. The third and following waves do not produce any inundation since the wave heights reduce, however, the sea level inside the bay still oscillates with considerable height (~ 2.0 m). Most of the return flow through the inlet of Wherowhero Lagoon and Waipaoa River had relatively high flow speed ~ 4.0 m/s (Figure 8.2.5.1-7.d).

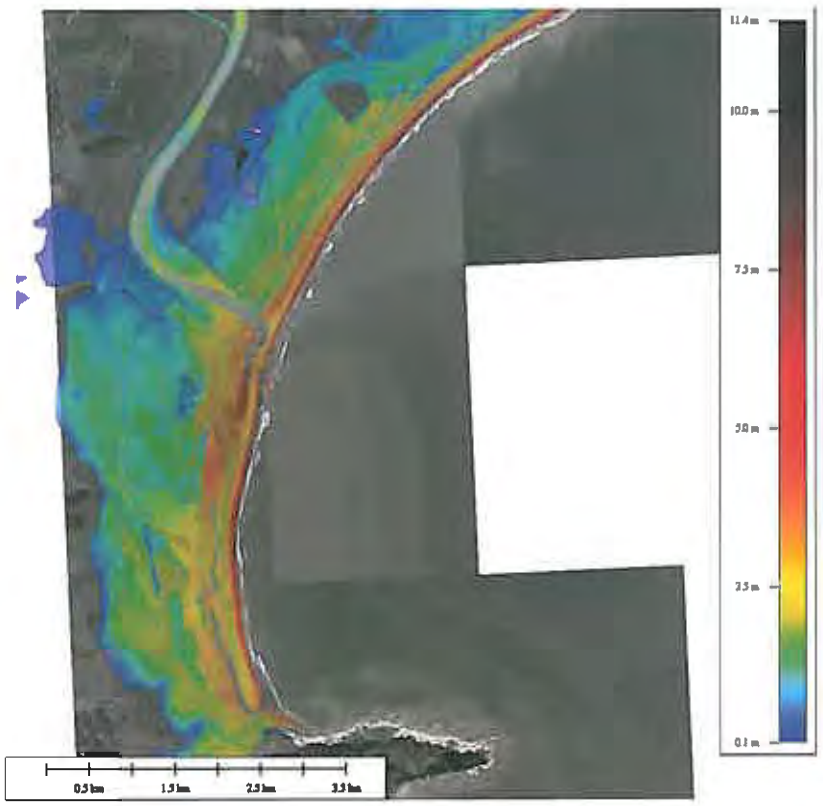

Figure 8.2.5.1-7 Maximum inundation and flow depth at Muriwai and adjacent shores (Mean Sea Level, Whole Margin Plate Interface, M_W 9.0).

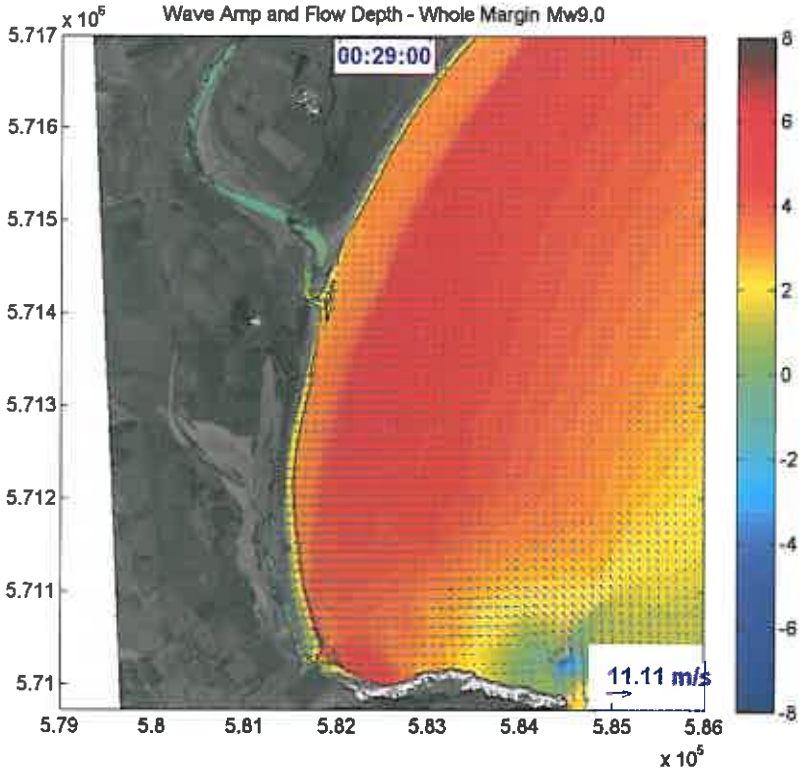

Figure 8.2.5.1-7.a Snapshot of tsunami propagation as it starts to inundate the Muriwai coastal area with an initial inundation occurring along the low-lying areas in front of Wherowhero Lagoon. The arrow in the lower right corner shows the scale for the velocity vectors. The scale bar is in metres.

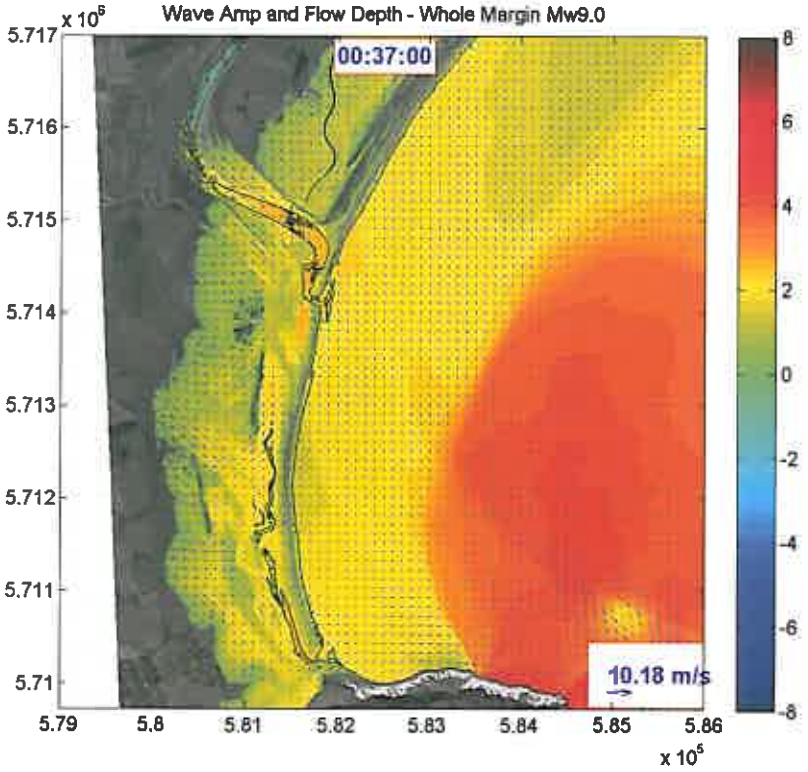

Figure 8.2.5.1-7.b Snapshot of tsunami that inundated the Wherowhero Lagoon, most of the Muriwai coastal area and the areas surrounding the Waipoa River. The arrow in the lower right corner shows the scale for the velocity vectors. The scale bar is in metres.

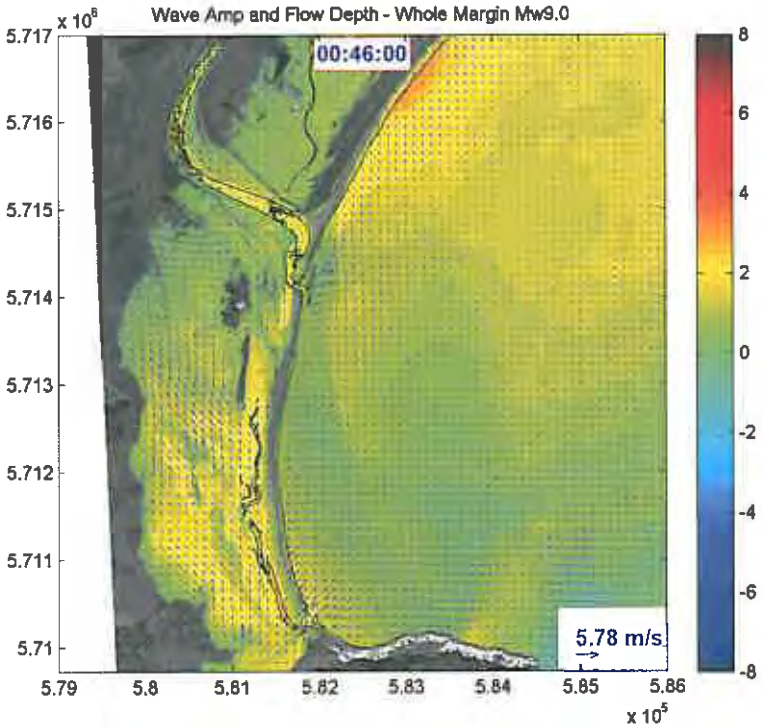

Figure 8.2.5.1-7.c Snapshot of a complex inundation pattern that occurs further inland due to local topographic features. Along the coast, the sand dunes prevent flow back to the sea. The inundation flows from Muriwai beach merge with the flows from the river mouth and creates further inundation inland. The arrow in the lower right corner shows the scale for the velocity vectors. The scale bar is in metres.

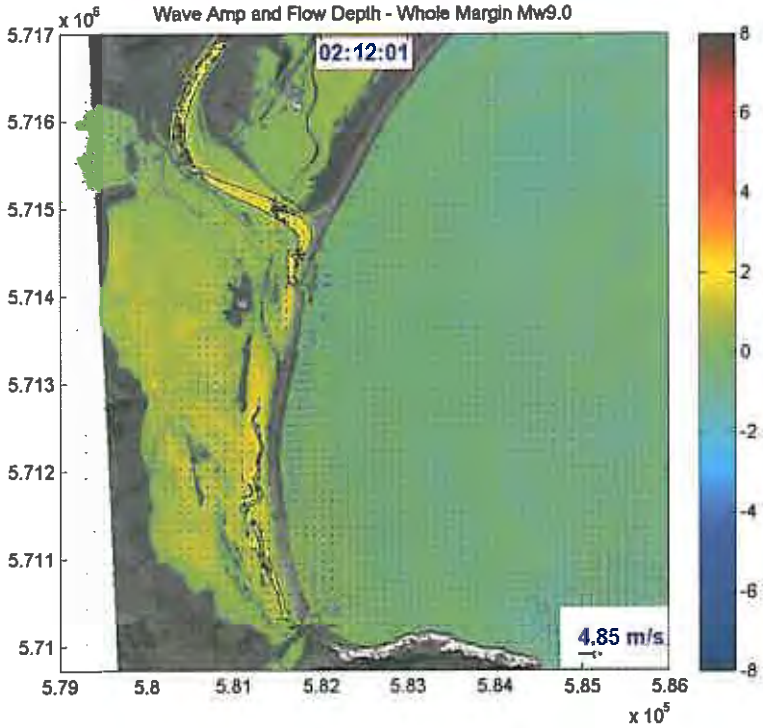

Figure 8.2.5.1-7.d Snapshot of tsunami inundation that shows the maximum inundation distance is the result of combined inundation flows from Muriwai Beach and the Waipaoa River. It shows also that the returning flow passes mostly through the Wherowhero Lagoon inlet and the Waipaoa River mouth since the sand dunes are high enough to divert the flow around them. The arrow in the lower right corner shows the scale for the velocity vectors. The scale bar is in metres.

8.2.5.2 *Model Results (scenario during the High Tide)*

In modelling the high tide condition, 0.75 m is added to the Mean Sea Level (MSL) as the tidal range in Poverty Bay is 1.5 m. The objective of this scenario is to assess the tsunami inundation dynamics during high tide. Model results show that increasing the sea level by 0.75 m produces profiles of incoming tsunami waves and patterns of water oscillations in the bay, that are very similar to those of the previous scenario. However, the maximum water levels in the Bay (gauge 3 and 7) and at the open coast (gauge 9) in comparison with the scenario for Mean Sea Level (Figure 8.2.5.2-1 and 2) are consistently increased by almost the same amount, 0.75 meters. This causes much more severe impacts in both the coastal areas of Gisborne City and the southwest side of Poverty Bay. Except for Wainui and section B, overtopping can be observed at most sand dunes, however, the extent of inundation further inland due to the increase of 0.75m in sea level is minor. The maximum inundation range and flow depth are shown in Figure 8.2.5.2-3.

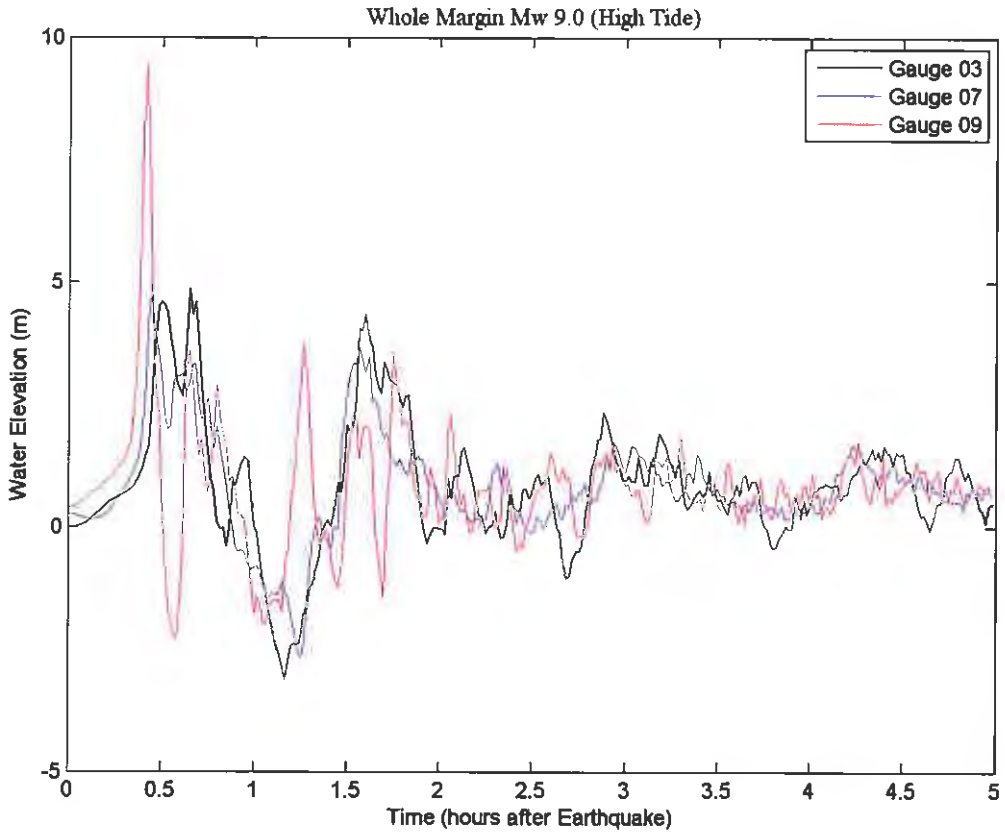

Figure 8.2.5-2.1 Water level fluctuations at virtual tidal gauges 03, 07 and 09 (high tide: 0.75 m above Mean Sea Level, Whole Margin Plate Interface, M_W 9.0) from the coast to offshore in the middle of Poverty Bay. This result also indicates an exceptional water level nearly 10.0 meters high near the Wainui coast (Gauge 09).

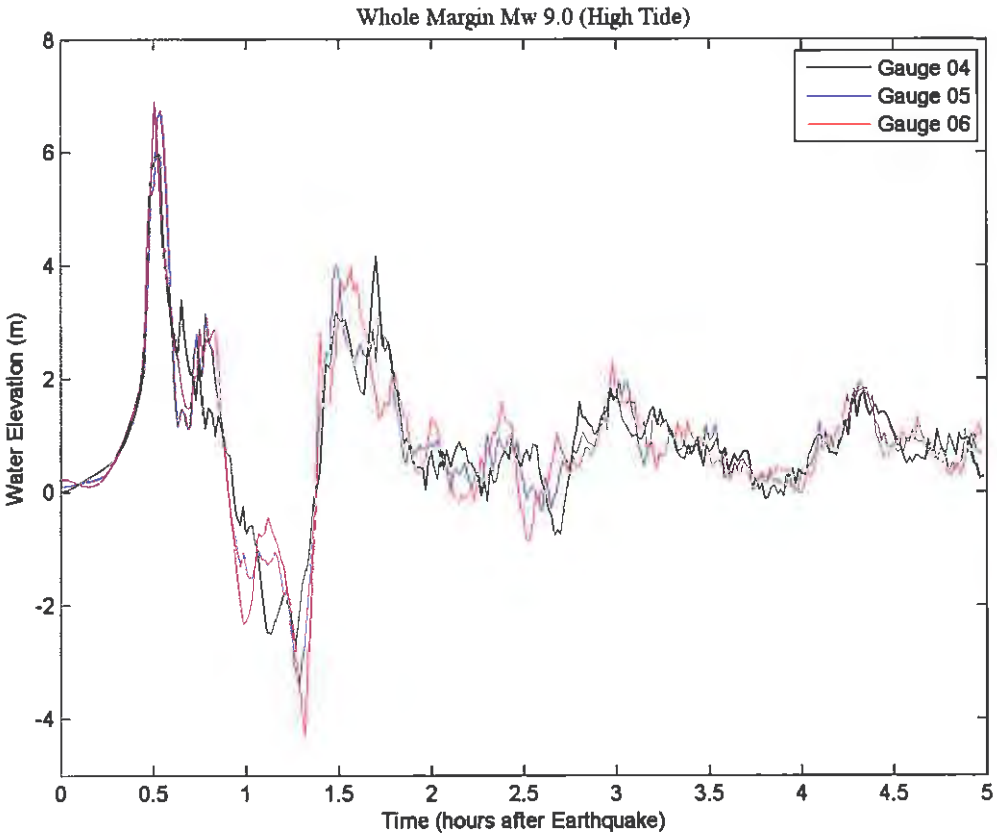

Figure 8.2.5.2-2 Water level fluctuations along the coast of Poverty Bay at virtual tidal gauges 04, 05 and 06; these show that waves arrive almost at the same time along the coast with almost the same height (high tide: 0.75 m above Mean Sea Level, Whole Margin Plate Interface, M_W 9.0).

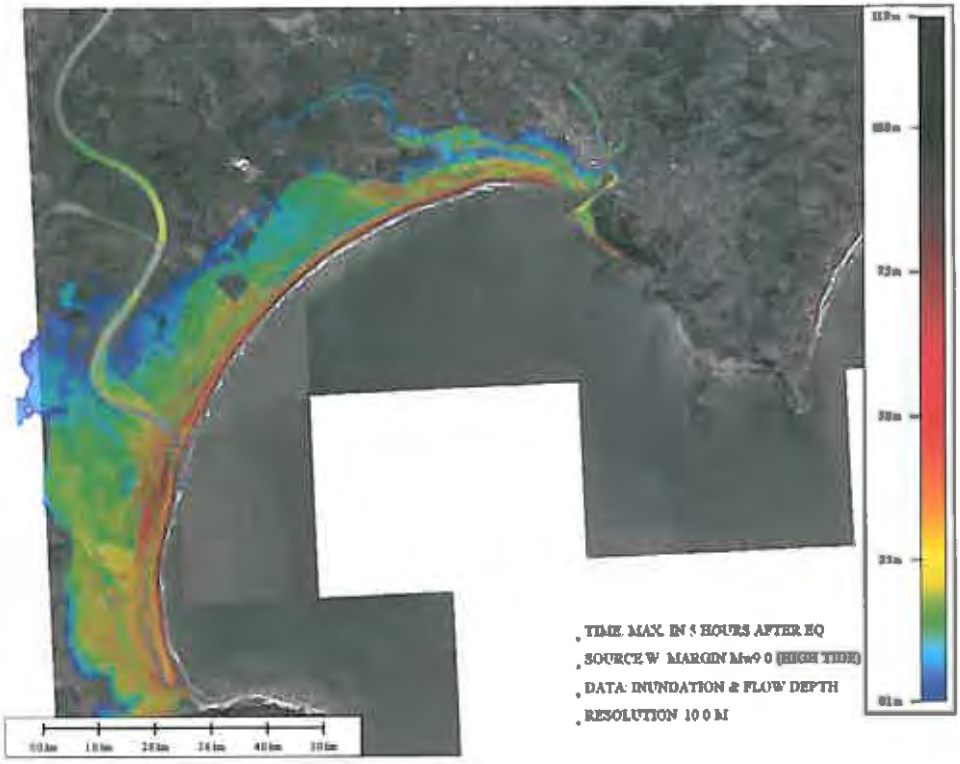

Figure 8.2.5.2-3 Maximum tsunami inundation and flow depth around Poverty Bay (high tide: 0.75 above Mean Sea Level, Whole Margin Plate Interface, M_W 9.0). The extent of tsunami inundation compared to the simulation at Mean Sea Level was greater in the areas behind Muriwai Beach and Waipaoa River and there were small changes inland to the areas behind the landfill.

Gisborne City

In this scenario, the tsunami inundates Gisborne City in a similar way to the scenario at Mean Sea Level. However, the flow depth is increased, and inundation is more severe and extends further inland. Victoria Domain is the limit of inundation for the area around the port and rivers, and the southern end of the airport runway is the limit for inundation that passed through Watson Park and the golf course (Figure 8.2.5.2-4)

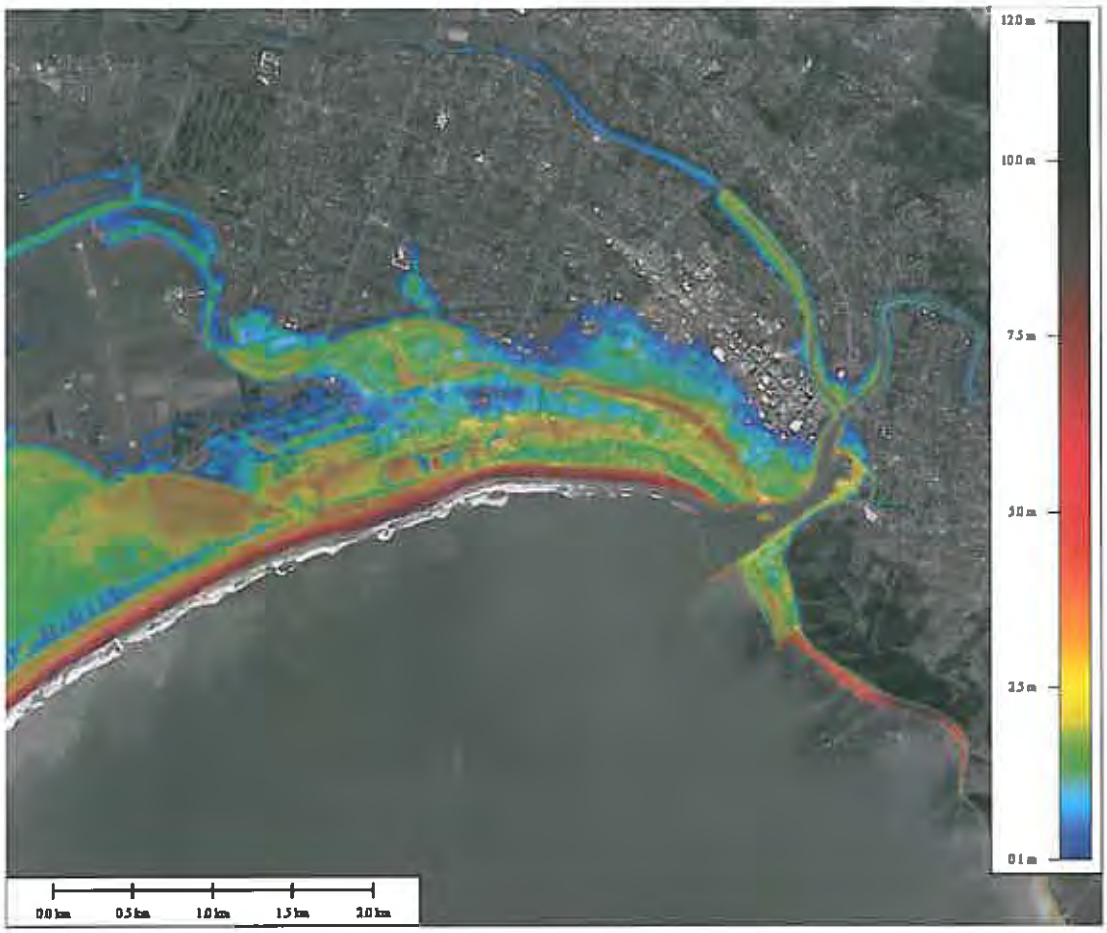

Figure 8.2.5.2-4 Maximum tsunami inundation and flow depth at Gisborne City and surrounding areas (High Tide, Whole Margin Plate Interface, M_W 9.0) shows that increasing the tide level, slightly increases the inundation height compared to the same magnitude at Mean Sea Level.

The sequential snapshots of tsunami inundation dynamics also show a similar pattern to the Mean Sea Level scenario. Tsunami flows hit the wharf and port facilities from the flow along the cliff of Titirangi Domain before most of the coastal areas around Poverty Bay are hit by the tsunami. The tsunami arrives a few minutes earlier compared to the Mean Sea Level Scenario (Figure 8.2.5.2-4.a and b). Tsunami inundation extends up to Victoria Domain due to the increase of flow depth that rushes up through Waikanae Creek, that is itself being pushed further inland by the flow coming from the seaside that overtops the sand dunes and passes through the access way to Grey Street (Figure 8.2.5.2-6, 7 and 8). Even though the flow depth increases, most of the areas surrounding the airport runway are still unaffected.

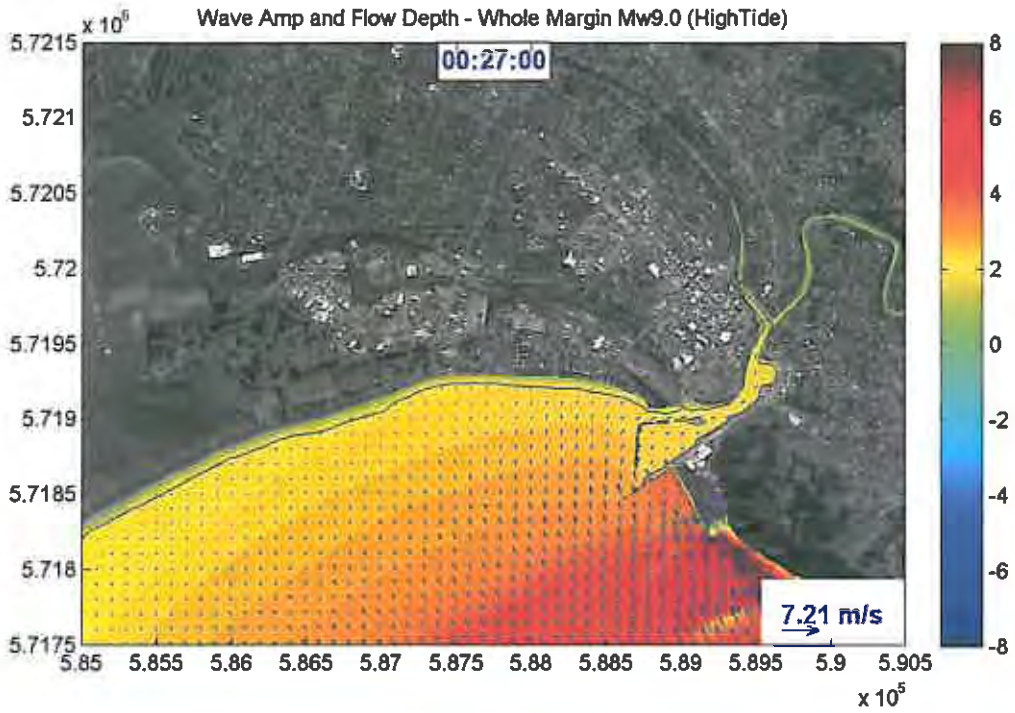

Figure 8.2.5.2-4.a Snapshot of tsunami propagation along the Cliff with high speed flows (~ 7 m/s) towards the Wharf. Increasing the tide level increases the flow speeds at this site. The arrow in the lower right corner shows the scale for the velocity vectors. The scale bar is in metres.

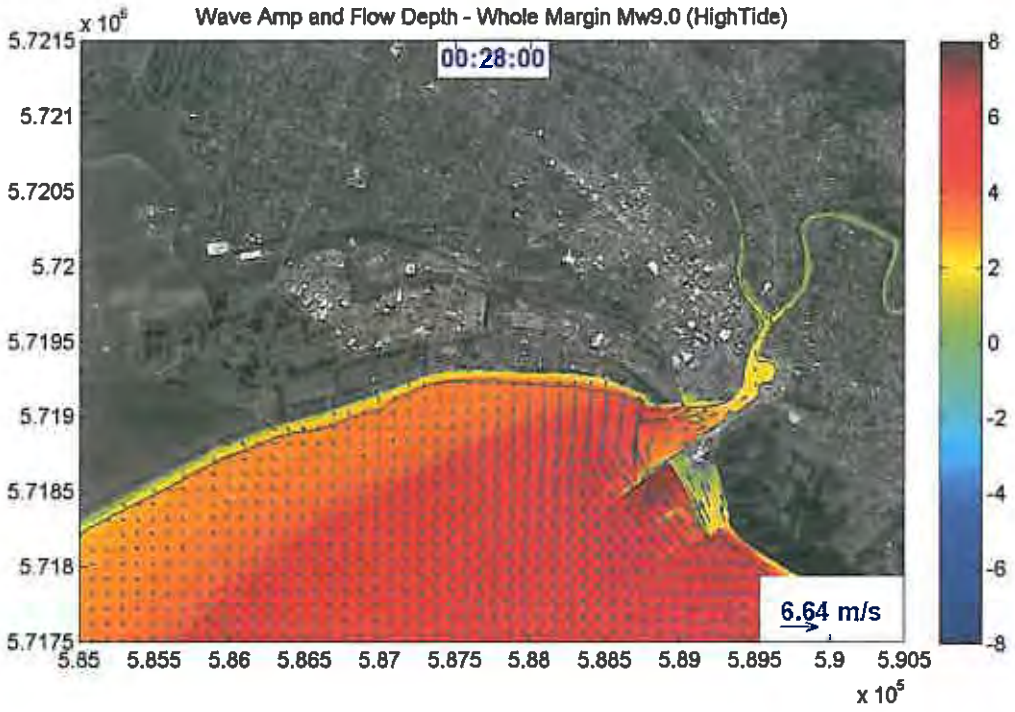

Figure 8.2.5.2-4.b Snapshot of tsunami over-washing the wharf, before overtopping the sand dunes along the coast. The arrow in the lower right corner shows the scale for the velocity vectors. The scale bar is in metres.

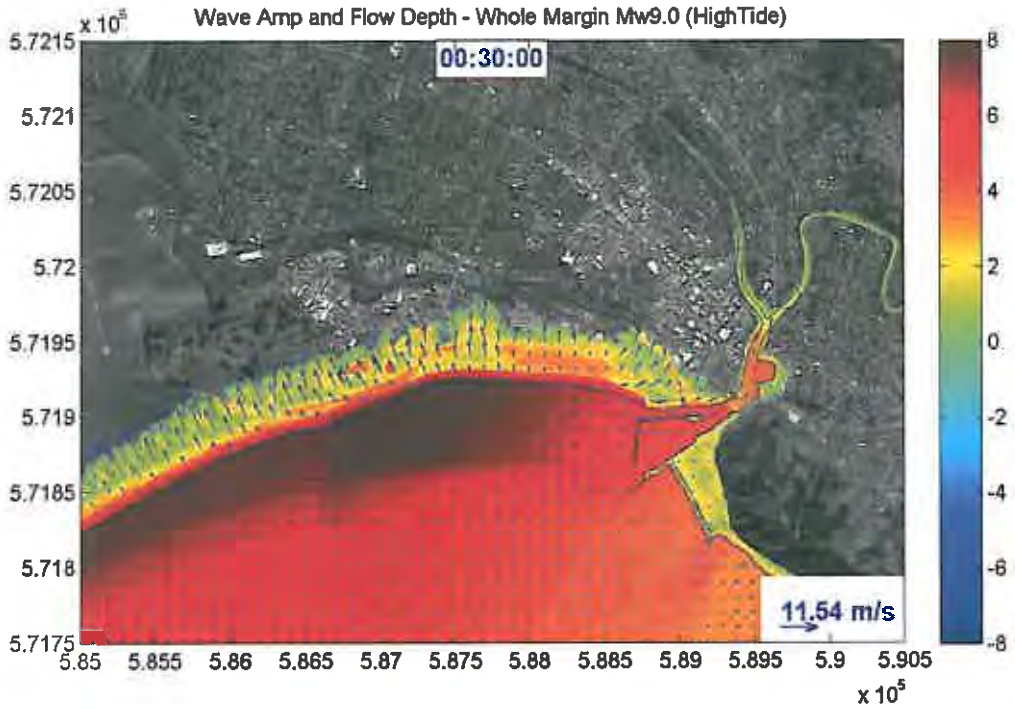

Figure 8.2.5.2-4.c Snapshot of inundation patterns during the first stages of inundation with unidirectional flows, with less effect of local topographical features. The arrow in the lower right corner shows the scale for the velocity vectors. The scale bar is in metres.

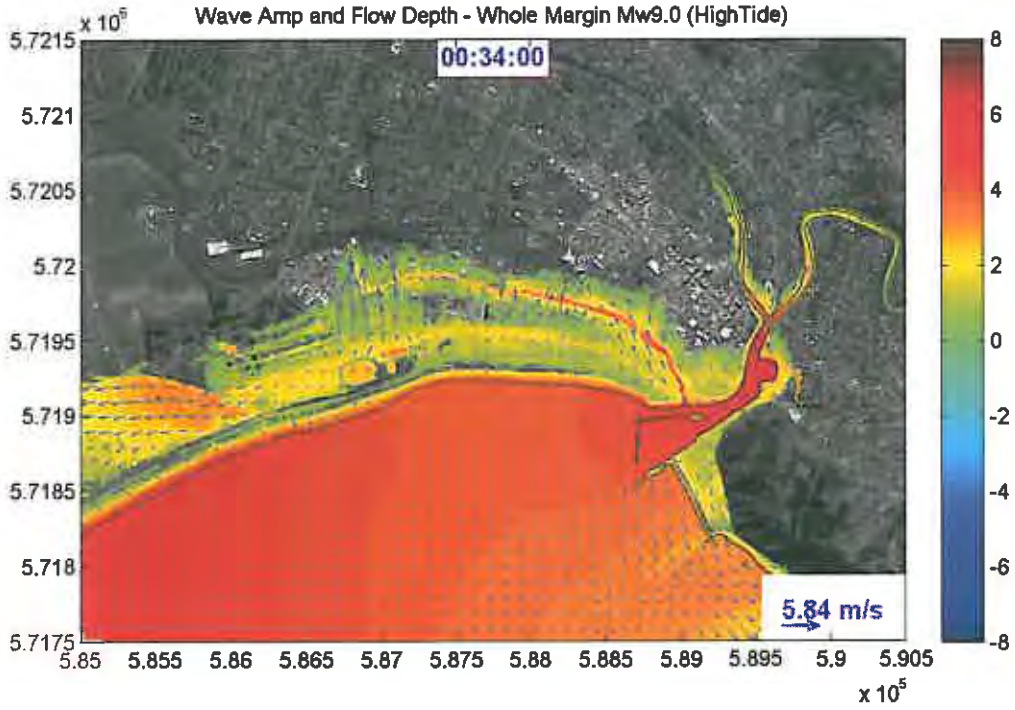

Figure 8.2.5.2-4.d Snapshot of inundation patterns further inland. While some of the seawater retreated through the low-lying areas, Waikanae Creek and Turanganui River as well as through the sand dunes gaps; increasing the water level by 0.75 m shows that the return flows could pass over some of the sand dunes along the coast. The arrow in the lower right corner shows the scale for the velocity vectors. The scale bar is in metres.

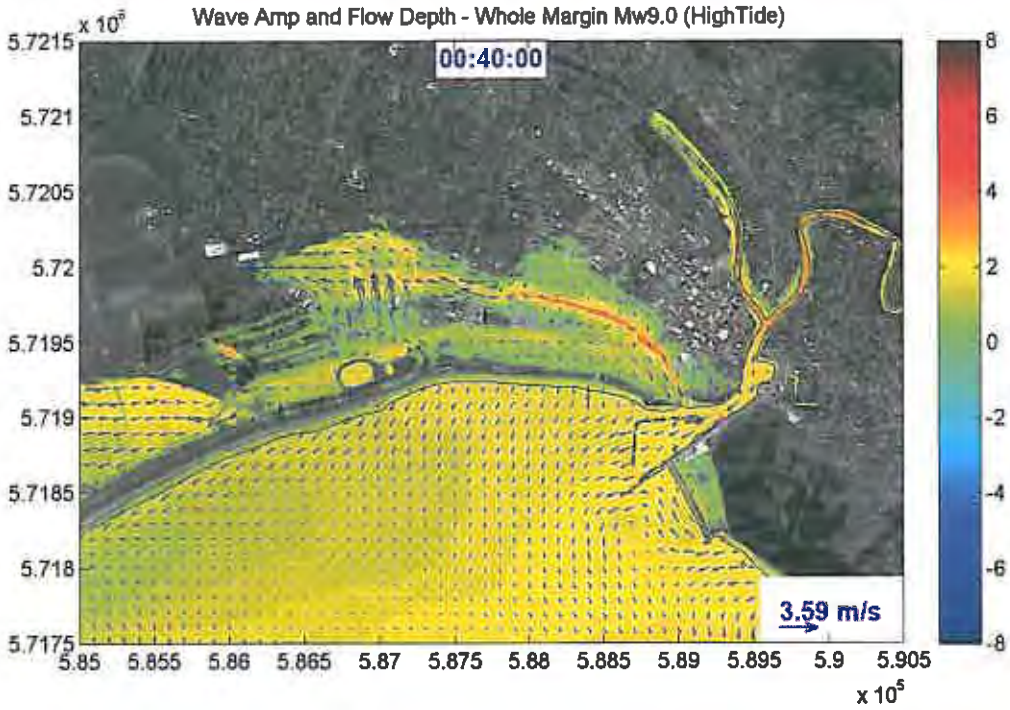

Figure 8.2.5.2-4.f Snapshot of further draining processes where most of the flows are through the low-lying areas and Waikanae Creek and Turanganui River since the dunes now act as a barrier. These flows create relatively strong currents outside the port, while flows in the Awapuni area are still moving further inland. The arrow in the lower right corner shows the scale for the velocity vectors.

Wainui

Twenty-two (22) minutes after the quake, tsunami with 4.0 m elevation arrives at the coast and inundates the beach front of the Wainui area (Figure 8.2.5.2-5). Within four minutes, the flow surges through the creek further upstream and inundates most of the low lying areas on both sides of the creek, mostly around the lower end of the creek close to the shore. The impacts of tsunami during this scenario compared to the scenario at mean tidal level are little different. The inundation flow comes from the creek at the northern end of Wainui Road and floods the road down towards the small creek in the middle of the Wainui area. Only the first waves inundate this region, and the inundation processes are very fast, taking less than 20 minutes for the tsunami to inundate further upstream and be drawn back to the sea (Figure 8. 2.5.2-5.a-d).

Figure 8.2.5.2-5 Maximum inundation and flow depth at Wainui (high tide: 0.75 m above Mean Sea Level, Whole Margin Plate Interface, M_W 9.0). The extent of inundation is slightly larger than the simulation results at Mean Sea Level. The arrow in the lower right corner shows the scale for the velocity vectors.

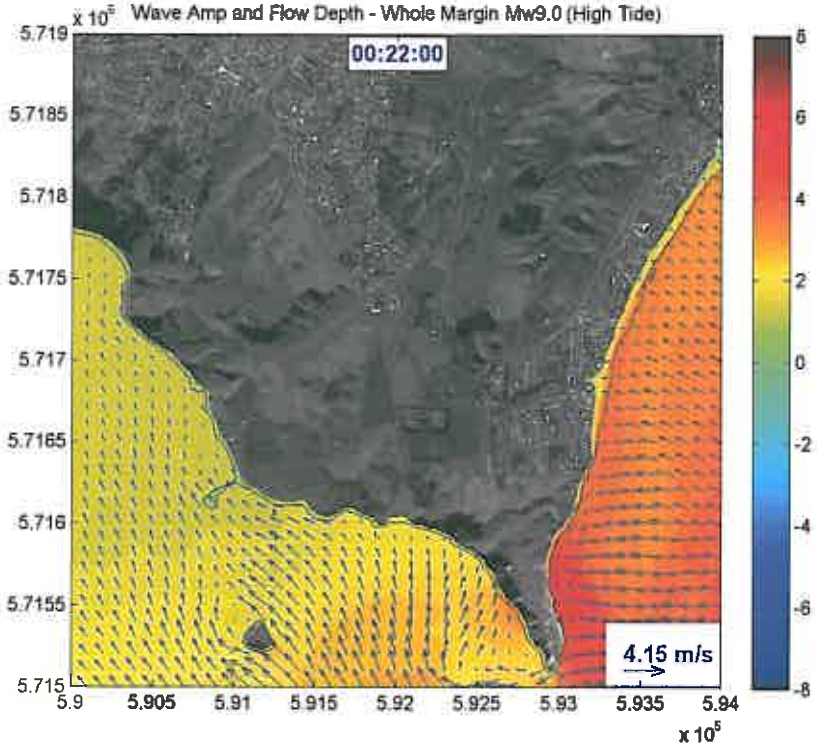

Figure 8.2.5.2-5.a Snapshot of tsunami that starts to inundate the Wainui coastal area. The arrow in the lower right corner shows the scale for the velocity vectors. The scale bar is in metres.

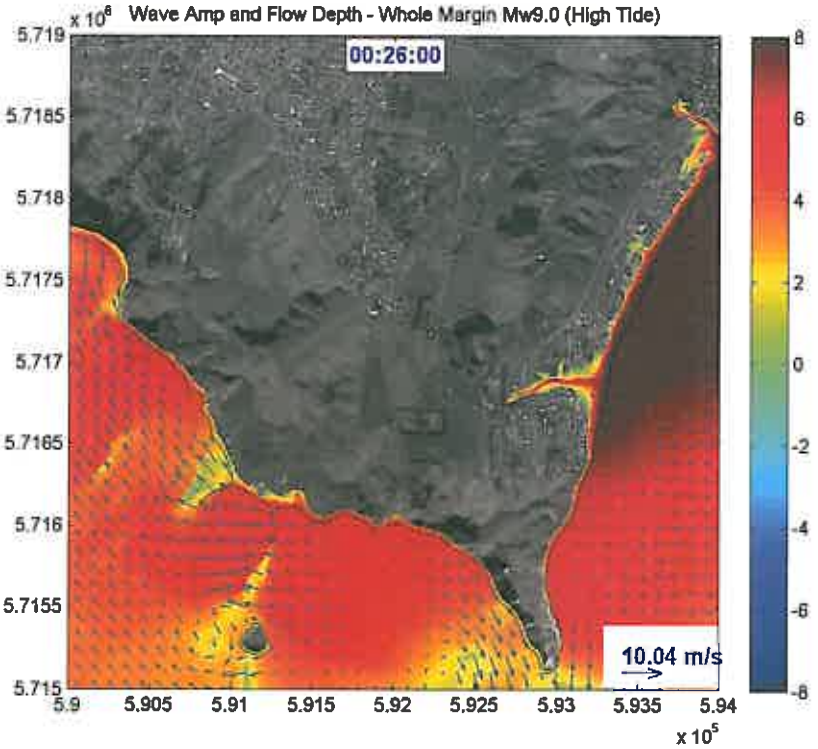

Figure 8.2.5.2-5.b Snapshot of tsunami that inundates the Wainui area via the creeks. The arrow in the lower right corner shows the scale for the velocity vectors.

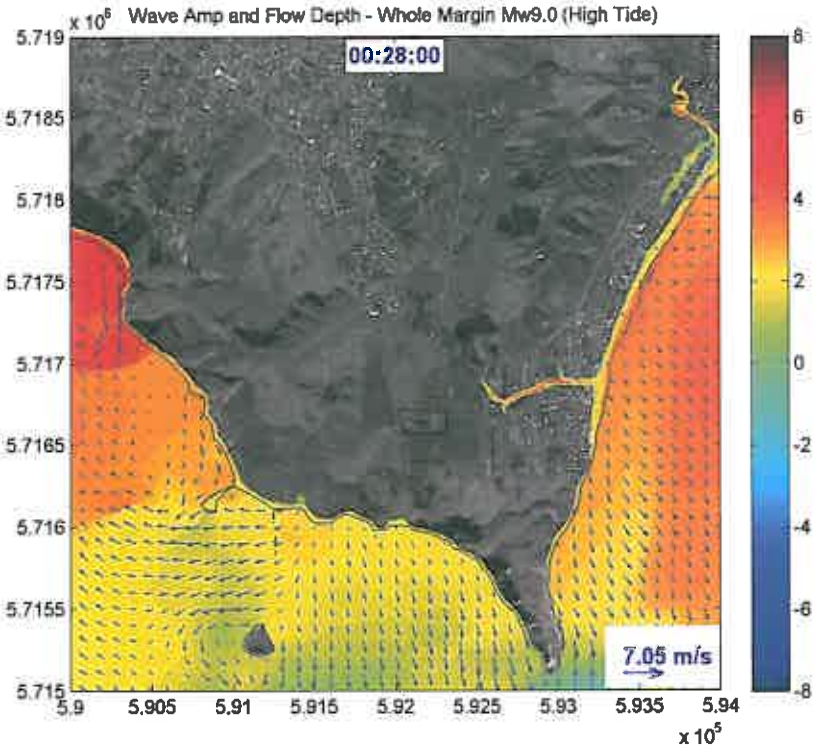

Figure 8.2.5.2-5.c Snapshot of tsunami during the returning flow. The arrow in the lower right corner shows the scale for the velocity vectors. The scale bar is in metres.

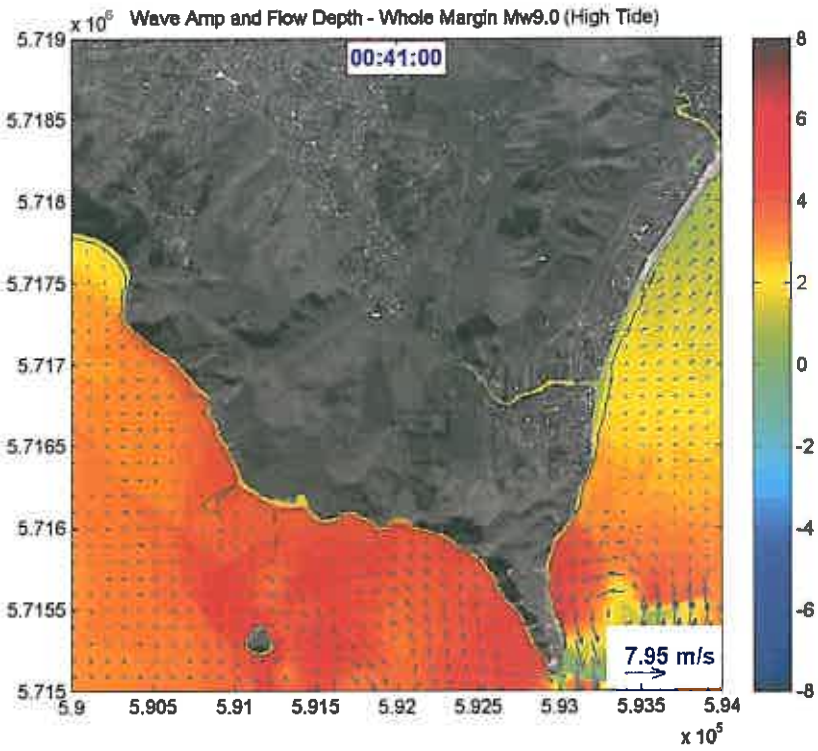

Figure 8.2.5.2.5.d Most of the seawater flows back to the sea within 20 minutes of the tsunami reaching its maximum inundation. The arrow in the lower right corner shows the scale for the velocity vectors. The scale bar is in metres.

Muriwai

A more severe inundation occurs of this low-lying region as shown by the model results with the inundation depth varying from 7.0 – 11.0 m along the coast and up to 1.0 – 4.0 m further inland (Figure 8.2.5.2-6). Increasing the sea level by 0.75 m (to represent high tide), increases the flow depth and extends the inundation distance. The areas behind Wherowhero Lagoon experience the same inundation distance inland as the Mean Sea Level scenario, as the increase of flow depth in this scenario is not enough to inundate the relatively high ground at this site. As a consequence, most of the flows are diverted to the north (Figure 8.2.5.2-6.a and b); hence increasing the inundation at the northern part behind the Waipaoa River. Even though most of the areas of this region are inundated, the dumping site (landfill) is still high enough to prevent the tsunami from overtopping. The inundation flows that come from the Waipaoa River mouth are very strong (with velocity of ~ 20.0 m/s), and within three minutes inundate the areas up to 1.5 km inland with the same flow path (Figure 8.2.5.2-6.c and d), and reach the Waipaoa River again. These strong flows are not following the river morphology even though they start from the river mouth.

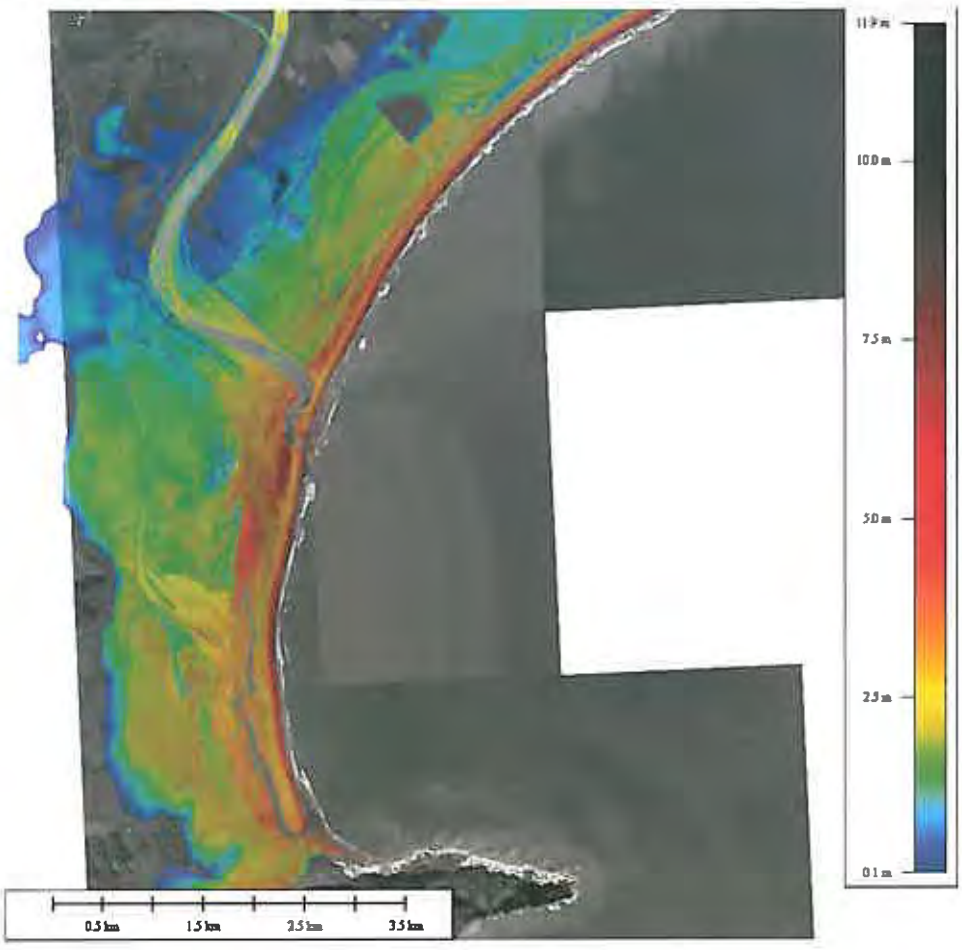

Figure 8.2.5.2-6 Maximum inundation and flow depth at Muriwai and adjacent shores (high tide: 0.75 m above Mean Sea Level, Whole Margin Plate Interface, M_W 9.0).

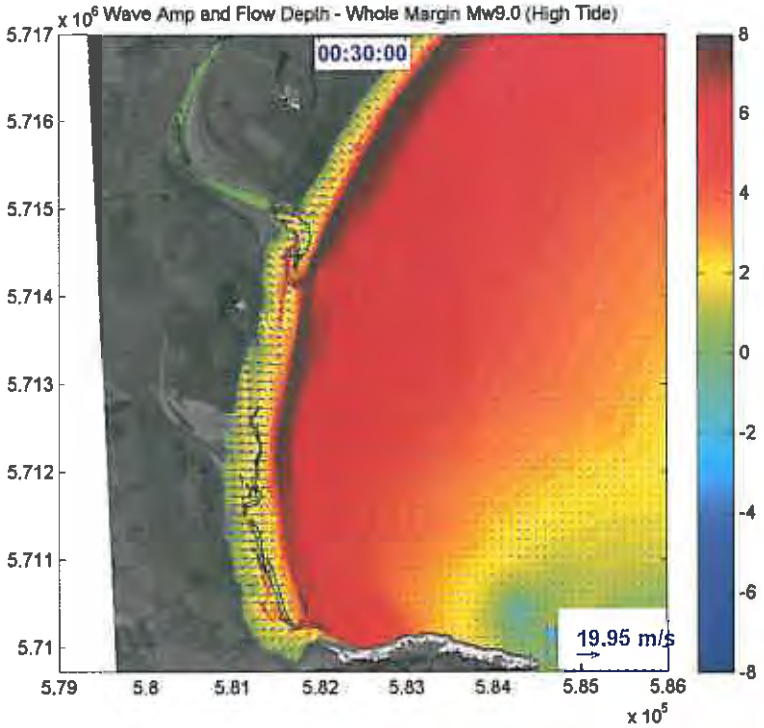

Figure 8.2.5.2-6.a Snapshot of the tsunami that starts to inundate further inland, overtopping most of the sand dunes including the areas in front of Waipaoa River that were not overtopped in the Mean Sea Level scenario. The arrow in the lower right corner shows the scale for the velocity vectors. The scale bar is in metres.

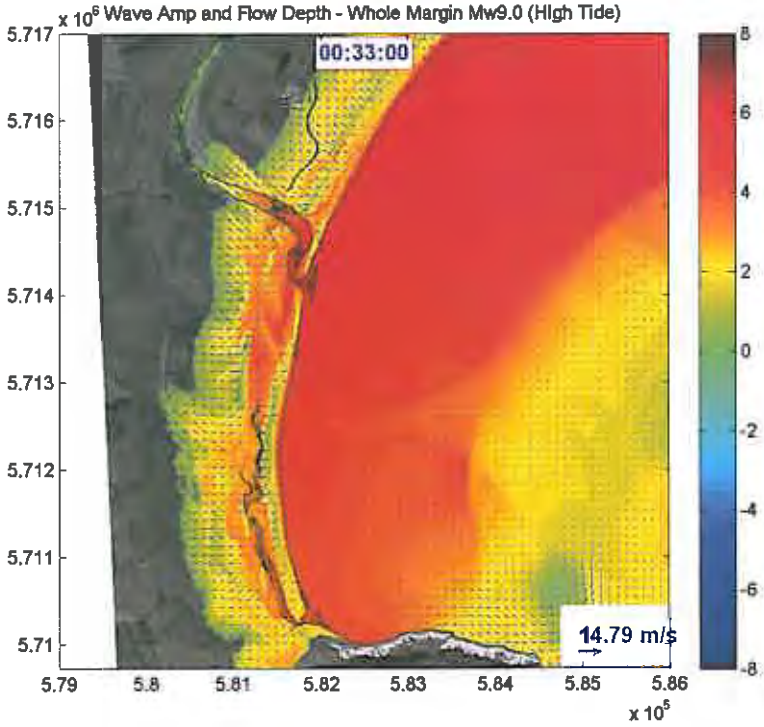

Figure 8.2.5.2-6.b Snapshot of tsunami inundation flows that shows the flow over Waipaoa Rivers occupying the river bank and most of the flow directions are the same as the flow direction when the tsunami starts to inundate the river mouth. In this region, increasing the water level according to the high tide level creates more severe inundation flows. The arrow in the lower right corner shows the scale for the velocity vectors.

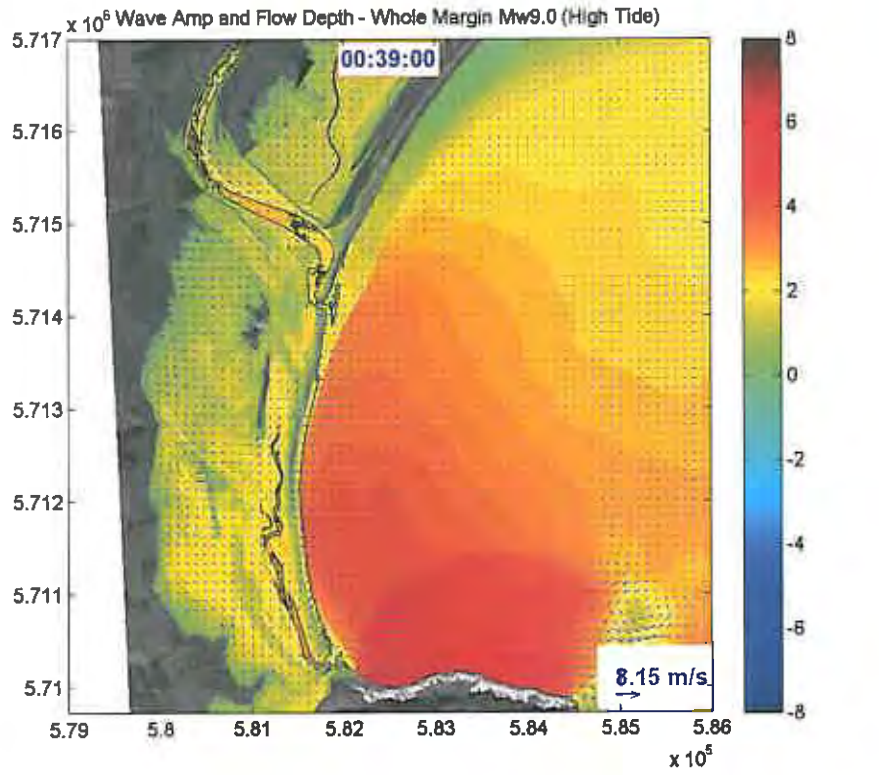

Figure 8.2.5.2-6.c Snapshot of the complex inundation pattern that occurs further inland where the flow from Muriwai beach merges with the flow from the river. The sand dunes along the coast at the northern side of the Waipaoa River are now exposed and hence most of the returning flows are diverted to the adjacent low-lying areas. The arrow in the lower right corner shows the scale for the velocity vectors.

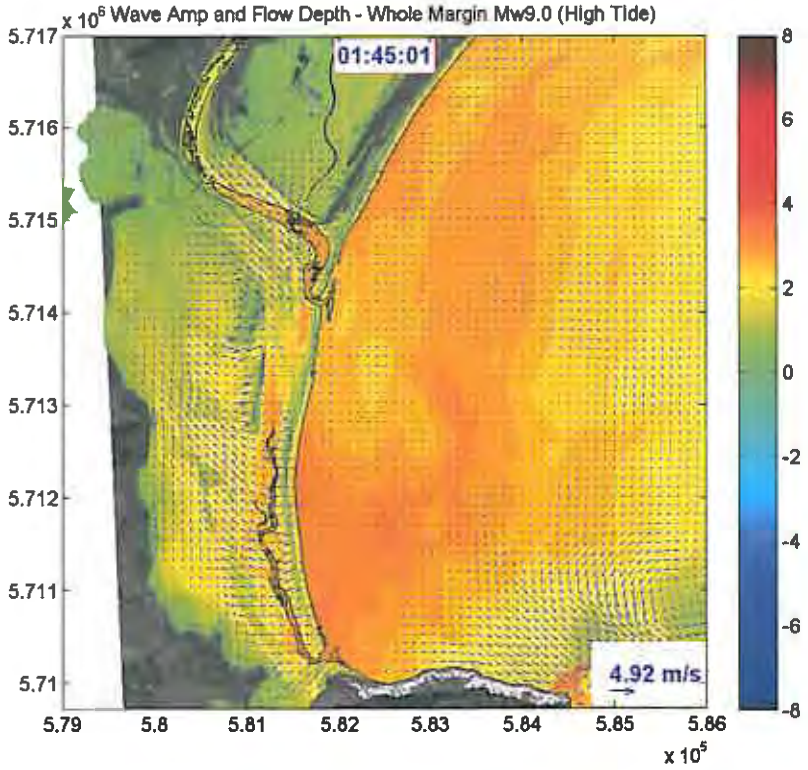

Figure 8.2.5.2-6.d The second wave follows the path of the first wave which inundates further inland most of the low-lying areas between Muriwai beach and the Waipaoa River. The arrow in the lower right corner shows the scale for the velocity vectors.

8.2.6 Whole margin plate interface M_W 8.8

The modelling results for this scenario show that along Poverty Bay, relatively significant inundation occurs to the low lying areas with a beach front height of less than 3.0 m (such as the low-lying areas of sections C and D), and minor inundation occurs to areas close to Gisborne City (section A) as well as to the Wainui area (Figure 8.2.6.-1). The time histories plot from the virtual tide gauges shows the wave profiles inside and outside the bay (Figure 8.2.6.-2 and – 3). The first tsunami wave with an elevation of ~ 6.0 m strikes along the coast of Poverty Bay, followed by the second wave about an hour later with a height of ~ 4.0 m. These waves can not overtop the sand dunes at section B, but inundate the rest of the bay to a certain level.

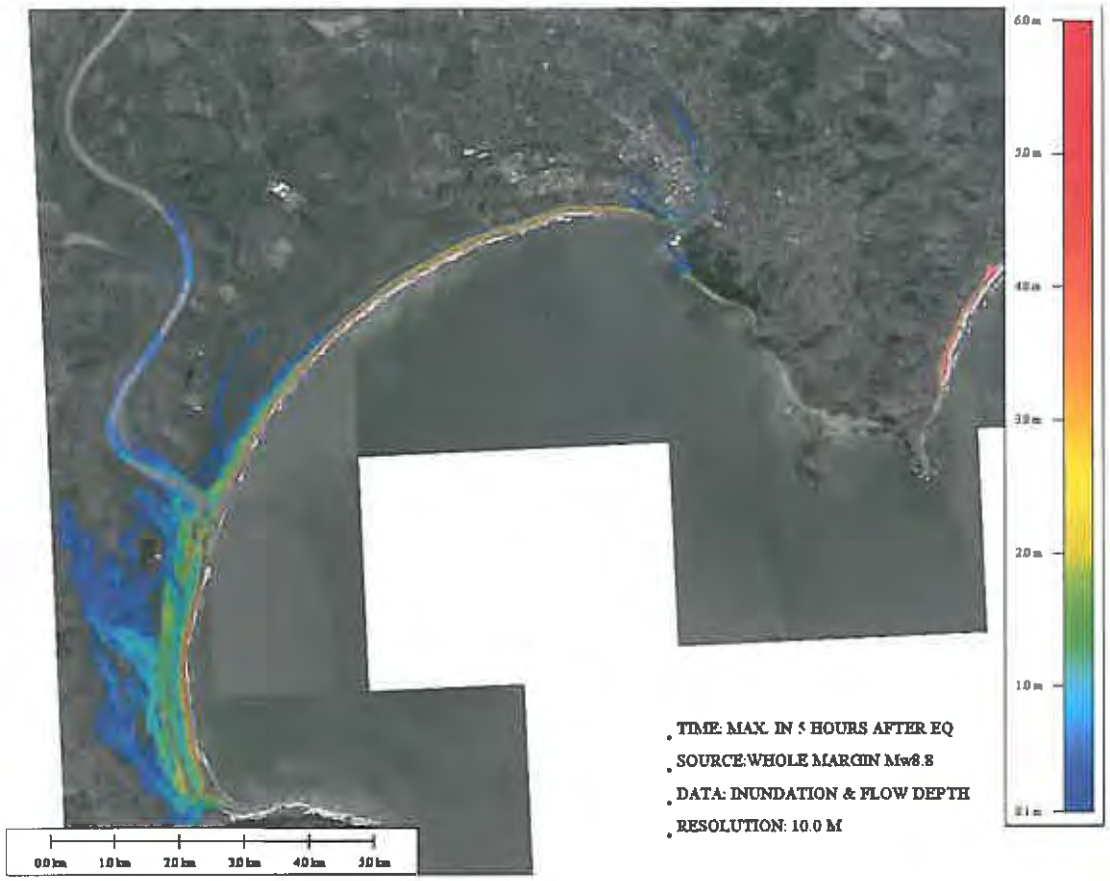

Figure 8.2.6.-1 Distribution of maximum tsunami inundation around Poverty Bay (Whole Margin Plate Interface M_W 8.8).

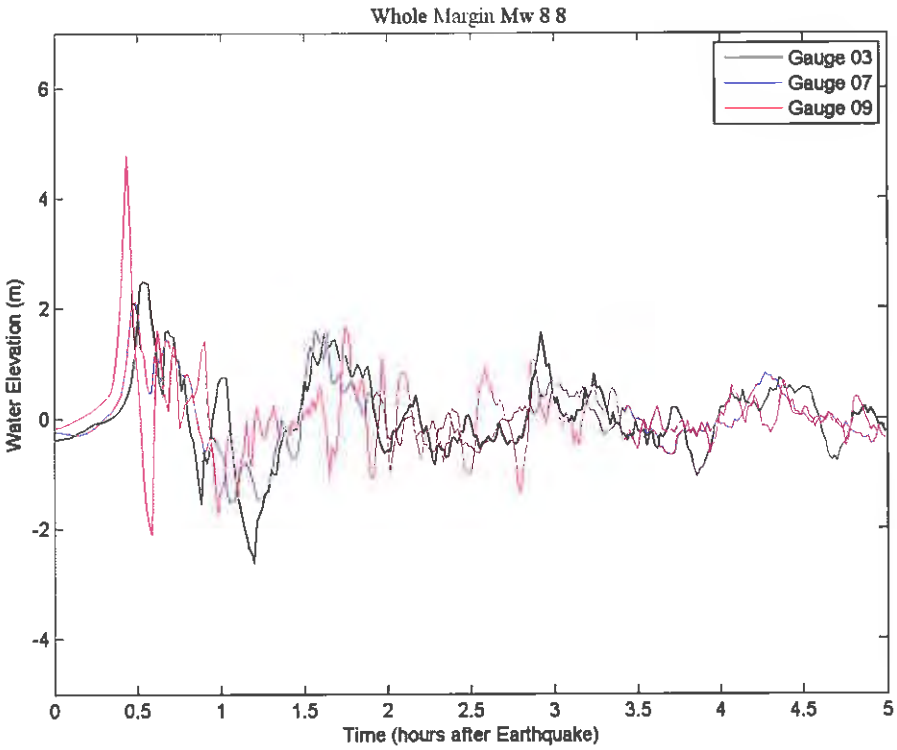

Figure 8.2.6.-2 Time histories plot (cross shore) in the middle of Poverty Bay.

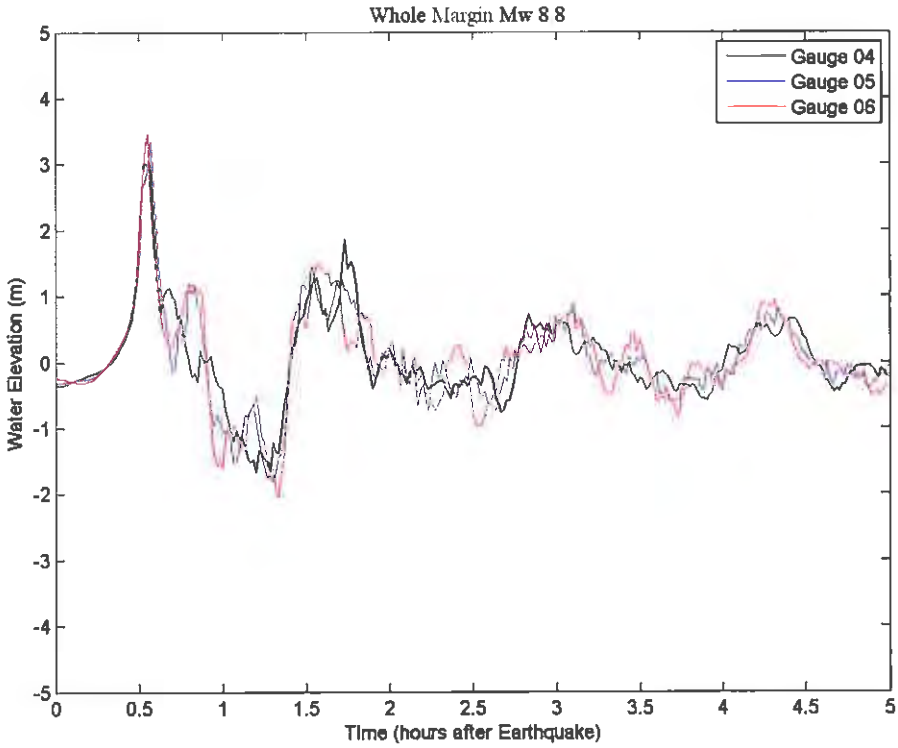

Figure 8.2.6-3 Time histories plot along the coast of Poverty Bay.

Gisborne City

The model results show that the access way at the end of Grey Street is the weakest point for this region as tsunami can more easily pass through the gap and inundate the neighbouring areas, although not severely (Figure 8.2.6.-4). The tsunami flow also rushes up the Waikanae Creek and Turanganui River as well as the Taruheru and Waimata Rivers. There is small flooding along the river banks. Maximum flow depth is ~ 1.0 m.

Figure 8.2.6.-4 Distribution of maximum tsunami inundation of Gisborne City.

Wainui

Minor inundation also occurs in this region, especially at the lower end of the creeks along the coast. The inundation does not create any harm to the residential areas along the coast (Figure 8.2.6.-5).

Figure 8.2.6.-5 Distribution of maximum tsunami inundation at Wainui.

Muriwai

As this region has a wide low-lying area with a beach front elevation of less than 1.0 m, it experiences a relatively moderate inundation. The tsunami inundates the lagoon after overtopping the sand spit and extends up to ~1 km inland with flow depths of 0.5 – 3.0 m (Figure 8.2.6.-6). Around the Waipaoa River mouth, the tsunami inundates most of this region but does not reach further inland. The tsunami does overtop the sand dunes immediately beyond the river mouth areas to the north, but the inundation flow does not go far inland.

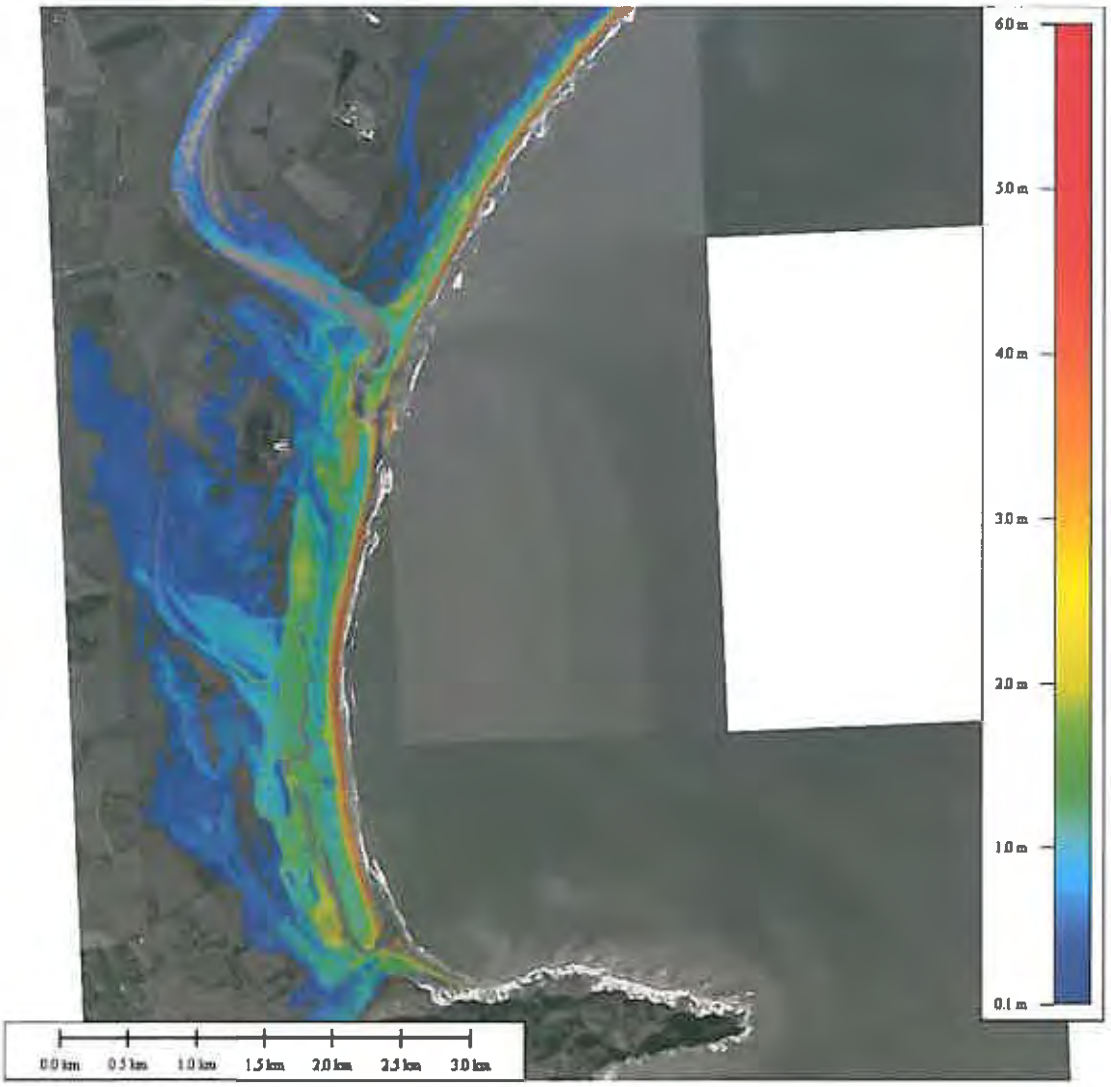

Figure 8.2.6.-6 Distribution of maximum tsunami inundation at Muriwai.

8.2.7 Outer Rise M_W 8.0

The modelling results show that the tsunami generated by the M_W 8.0 Raukumara Outer Rise source model is not able to result in obvious inundation in the city area of Gisborne and only minor inundation can be found in the area of Wherowhero Lagoon (Figure 8.2.7-1). The maximum amplitude of water fluctuations inside the bay is around 2.0 meters. However, unlike all the previous scenarios, a depression-type leading wave is generated and observed inside the bay (Figure 8.2.7-2). Although the tsunami in this scenario is not able to cause obvious inundation in the city area of Gisborne and only a small amount of inundation is found in the area of Wherowhero lagoon, much more severe flooding along the coastal areas of Wainui can be found from the modelling results. Possible reasons for this include the orientation of the source relative to the Wainui coast, and the different period of waves from this source.

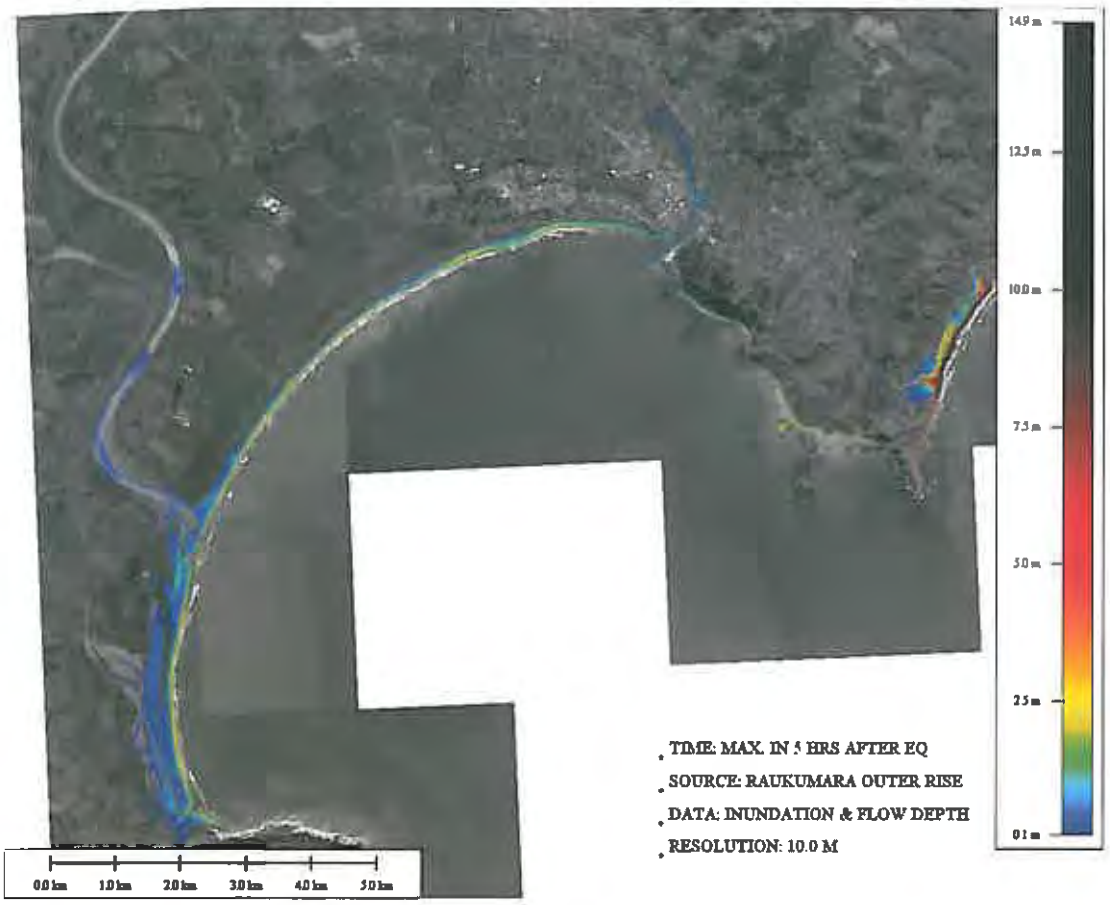

Figure 8.2.7-1 Maximum inundation and flow depth of the tsunami generated by the M_W 8.0 Outer Rise source model. Only minor inundation can be observed in the area of Wherowhero Lagoon at the southwest side of Poverty Bay. However, much more severe flooding is found along the coast of Wainui.

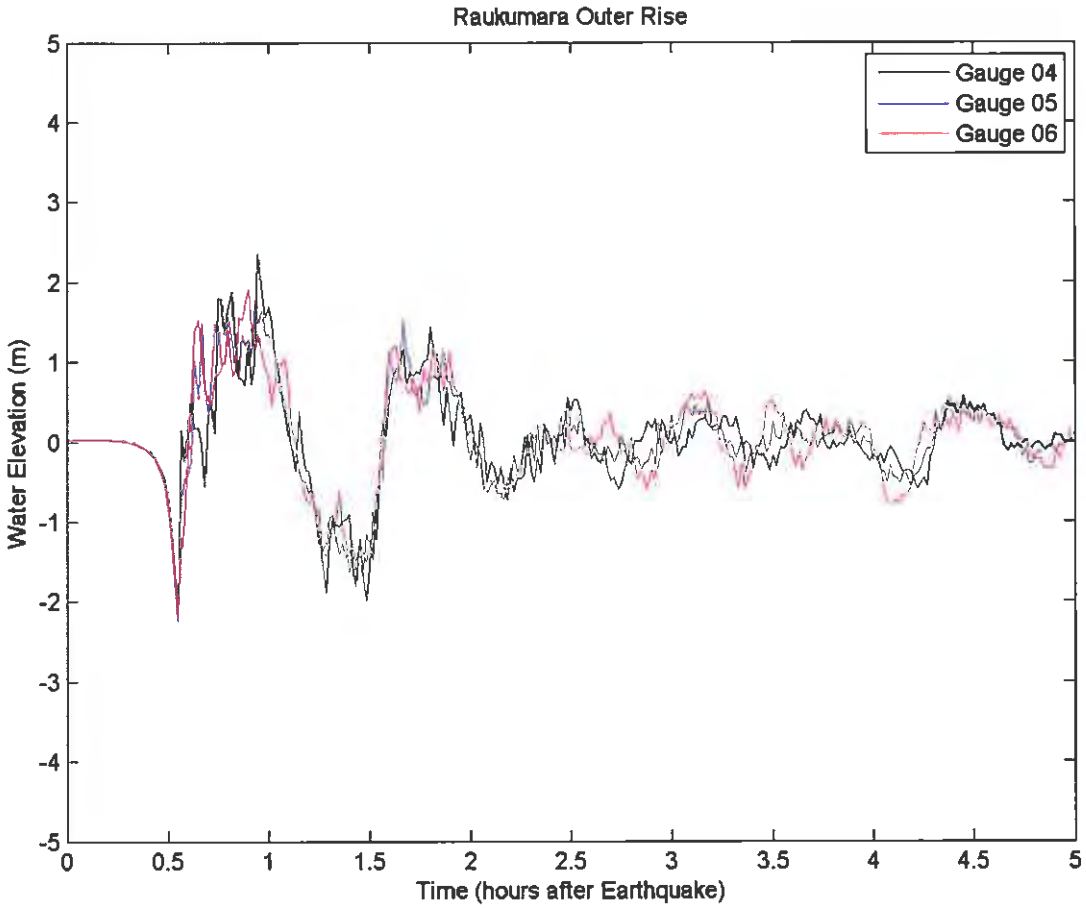

Figure 8.2.7-2 Time history records at virtual tidal gauge 04, 05 and 06, just in front of the sand dunes encompassing Poverty Bay.

Numerical modelling shows that most residential areas along the coast of Wainui are flooded during this event, with inundation range up to 500 m inland. On the beach front, 10.0 ~ 15.0 meter flow depth is observed from the modelling results. In the residential areas along Wairere Road, flow depths may reach up to 2.0 ~ 3.0 meters (Figure 8.2.7-3).

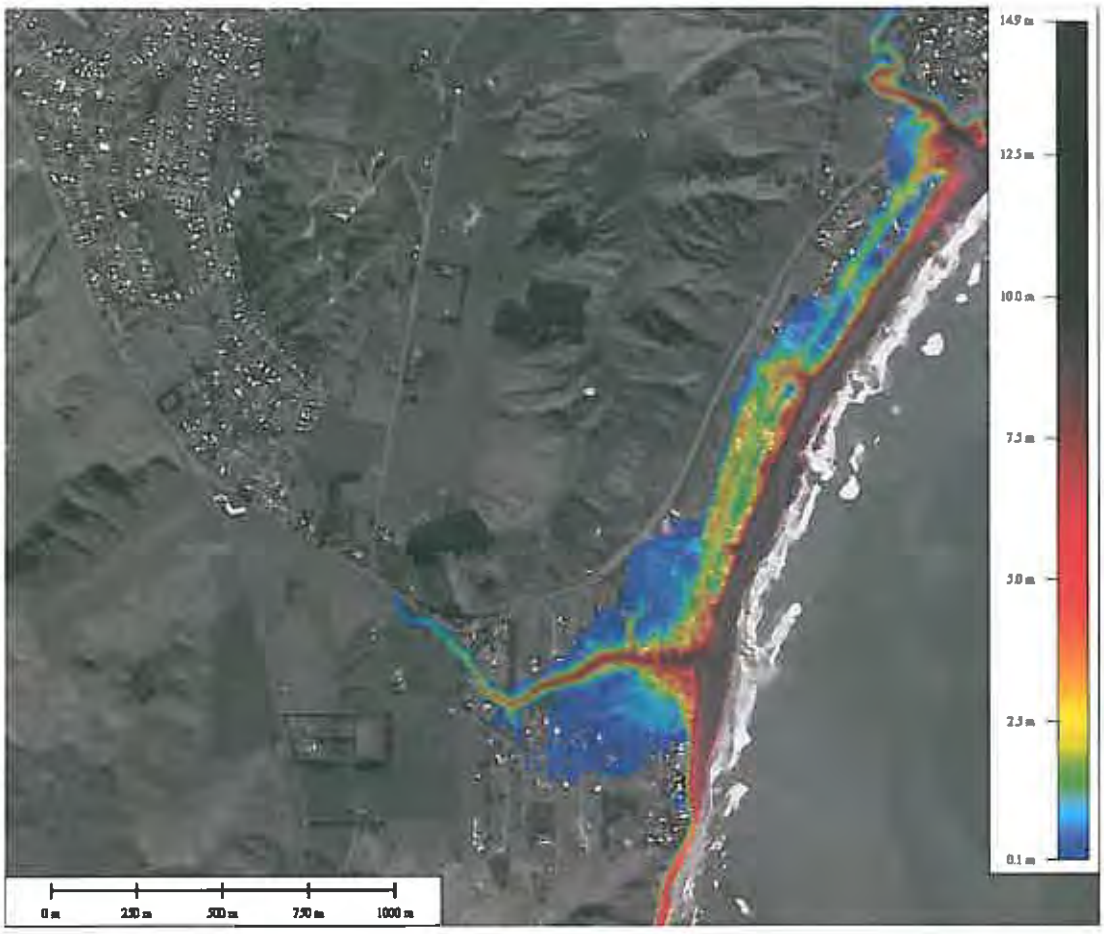

Figure 8.2.7-3 Maximum inundation and flow depth in the costal areas of Wainui, caused by the tsunami generated by the Outer Rise source model

8.2.8 Gisborne segment rupture

The modelling results show that the tsunami generated by the rupture of the Gisborne fault segment is not capable of causing significant threats to the coastal areas of Gisborne City and Wainui. In this scenario, although the water fluctuations may reach about 4.0 meters above Mean Sea Level, the entire Poverty Bay area is also uplifted 1.0 to 2.0 meters by the earthquake (Figure 6.2.8-1, 8.2.8-1 and 8.2.8-2). The modelling results demonstrate that strong surges of water, up to 2.0 ~ 3.0 meters high are expected to flood into the mouth of Turanganui River and travel upstream, but no significant inundation can be observed. In contrast, at the southwest of the bay, this scenario results in severe inundation over about 2.0 km inland (Figure 8.2.8-3). The flow depth may range from 1.0 to 3.0 meters.

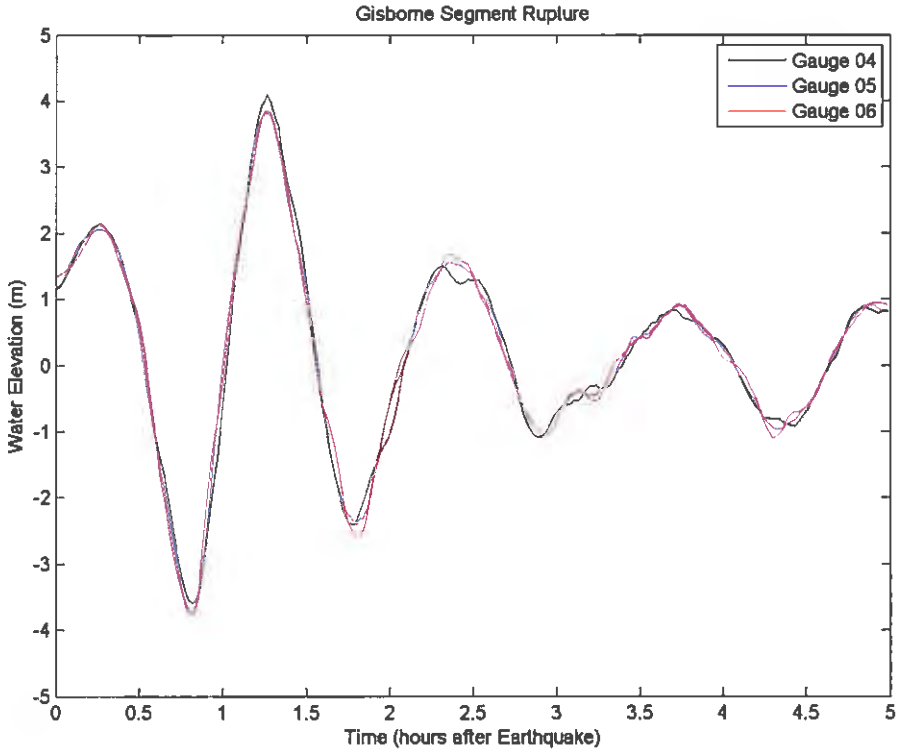

Figure 8.2.8-1 Time history records along the coast of Poverty Bay at virtual tidal gauges 04, 05 and 06. The tidal records imply that, the seafloor is uplifted over 1.2 meters at gauges 04 and 05, and about 1.4 meters at gauge 06 by the earthquake.

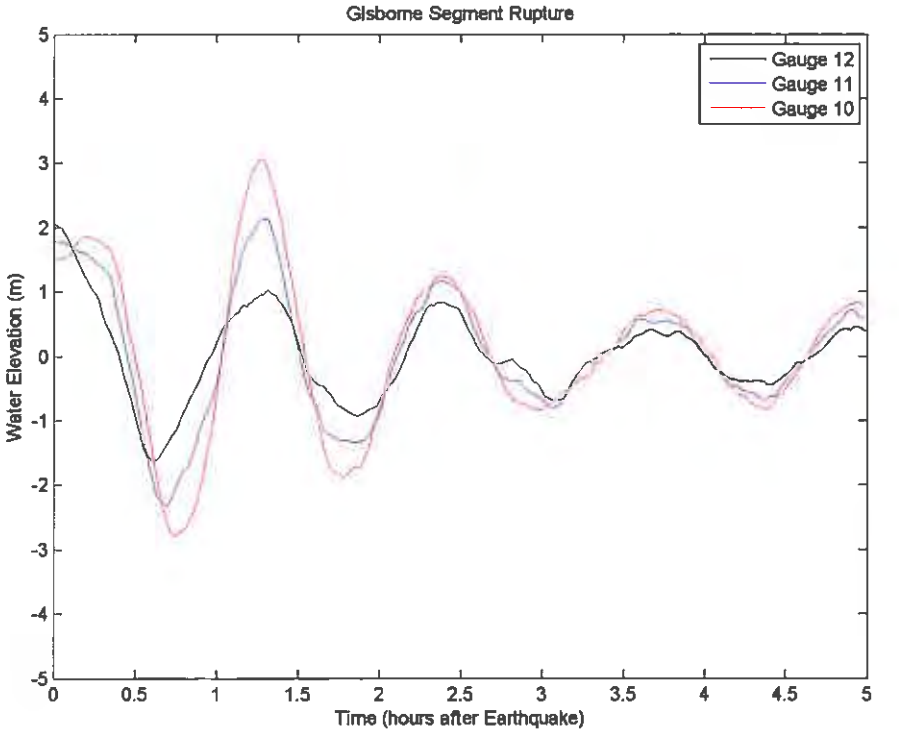

Figure 8.2.8-2 Time history records in the middle of Poverty Bay at virtual tidal gauges 10, 11 and 12. The tidal records imply that the seafloor of Poverty Bay is uplifted 1.0 metre at gauge 10, 1.5 metres at Gauge 11 and over 2.0 metres at gauge 12.

Figure 8.2.8-3 Maximum inundation and flow depth caused by tsunami generated by Gisborne Segment rupture (M_W 7.8). The modelling results show severe flooding at the southwest side of Poverty Bay.

8.2.9 Interface rupture based on GPS coupling

In this source model, an M_W 8.1 earthquake event was derived from GPS observations of the slip rate deficit due to plate coupling, and a 400 year recurrence interval was assumed to determine the slip amount. The modelling results show that this M_W 8.1 earthquake event is not able to generate tsunami significantly threatening to the coastal areas encompassing Poverty Bay. The amplitude of water fluctuations in the bay caused by this tsunami is usually below 1.5 m (Figure 8.2.9-1). This magnitude of tsunami waves is not capable of inundating the Gisborne City area and Wainui, and from the numerical modelling only minor inundation is observed in the area of Wherowhero Lagoon, southwest of Poverty Bay (Figure 8.2.9-2).

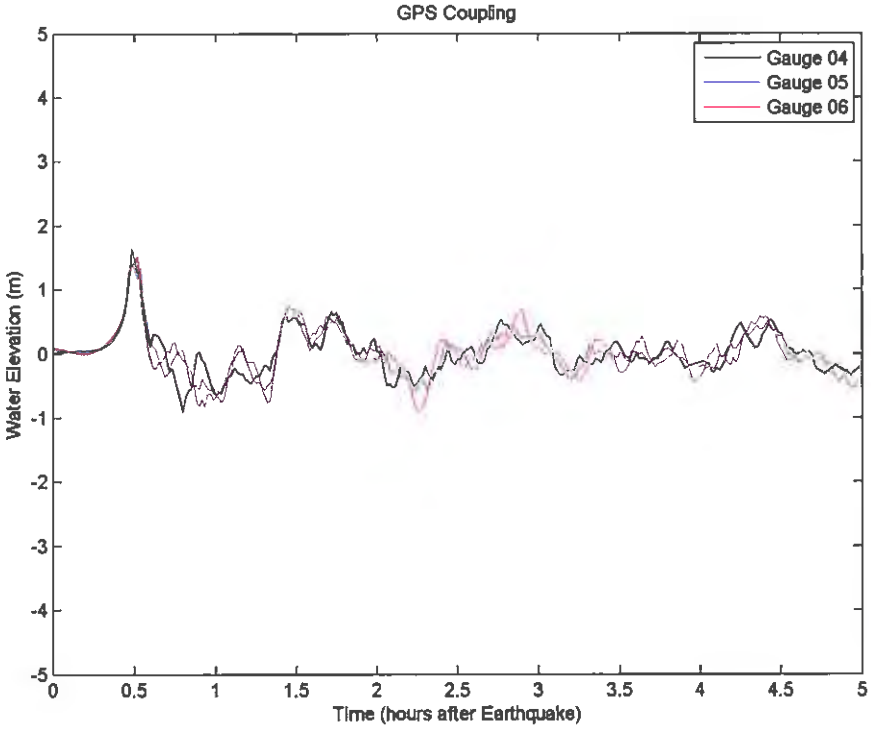

Figure 8.2.9-1 Time history records along the coast of Poverty Bay at virtual tidal gauges 04, 05 and 06. The tidal records show that in the coastal areas in front of the sand dunes, the amplitude of water fluctuations is below 1.5 meters.

Figure 8.2.9-2 Maximum inundation and flow depth caused by tsunami generated by the earthquake derived from GPS coupling (M_W 8.1). The modelling results show only minor inundation in the area of Wherowhero Lagoon, southwest of Poverty Bay.

8.3 Return times for tsunami inundation

For evacuation and land-use planning it is often useful to think in terms of the return time of a particular impact at a given site. For example, if we estimate that on average a given small patch of land is inundated by tsunami every 200 years, then we can say that the return time for tsunami inundation at that location is 200 years.

Many different sources may contribute to the tsunami hazard at any particular return time, and individually these sources may have much longer recurrence intervals (the recurrence interval is the average length of time between consecutive source events of a given type). For example, if there were three main sources with similar impacts, each of which has a recurrence interval of 300 years, then collectively they would contribute to the 100 year return time for inundation.

Estimating the return time for tsunami inundation is a very difficult process requiring a comprehensive set of models for all the scenarios which contribute to the tsunami hazard on the time scales of interest, and a model for the probabilities of each scenario. The set of scenarios modelled for this study, and their recurrence interval estimates, are not sufficient to perform such an analysis in a systematic way.

However using expert judgement we will attempt to discuss the implications of our scenario results for tsunami hazard at some key return times of interest.

8.3.1 Distant sources

The impact of distant tsunami sources is less sensitive to the details of the source than is the case for local sources (Geist, 1998). With this in mind we chose two scenarios with the intention that they approximately represent the extent of the 100 year and 500 year return-time tsunami inundations.

Table 8.3.1-1 Distant sources contributing to the tsunami hazard at different return times.

Return time	**Sources contributing to tsunami hazard**
<100 years	Peru & Central America $M_W \leq 9.1$ Other Pacific Rim $M_W \leq 9.4$
100 – 500 years	Peru $M_W \leq 9.4$ Other Pacific Rim $M_W \leq 9.5$
500 years – 2500 years	Peru $M_W \leq 9.5$

8.3.2 Local sources

The inundation caused by local sources can be very specific to the details of the source (Geist, 1998), and these details are usually not known with confidence. In general we cannot pick out a single scenario and use the inundation in that event as representative of the inundation extent at a given return time.

Table 8.3.2-1 Local sources contributing to the tsunami hazard at different return times. The sources indicated with a question mark may not occur, but cannot be ruled out with 84% confidence (the standard criteria for issues of life safety).

Return time	Sources contributing to tsunami hazard
<100 years	Tsunami earthquakes, similar to March & May 1947 tsunami
100 – 500 years	Earthquakes on subduction-zone splay faults (Lachlan, Ariel Bank, Gable End) possibly with slip on the deeper plate interface. Plate interface earthquakes (Raukumara & Hawke's Bay region) $M_W \leq 8.1$ Tsunami earthquakes larger than March 1947?
500 years – 2500 years	Outer Rise earthquakes Plate interface earthquakes (Raukumara & Hawke's Bay region) $M_W \leq 8.5$? Whole margin ruptures $M_W \leq 9.0$? Landslide sources?

At the 100 year return time the inundations from the March and May 1947 events can provide a rough guide to the extent of inundation. These scenarios were not modelled, but the historical impacts are well known and provide the best available guide.

At the 500 year return time the Lachlan Fault with deeper plate interface scenario probably comes closest to representing the extent of inundation within Poverty Bay. For Wainui a scenario of an Ariel Bank with deeper plate interface earthquake (not currently modelled), may be more appropriate on that coast.

At the 2500 year return time, and taking into account the need to consider scenarios that cannot be confidently ruled out, the M_W 9.0 whole margin scenario probably comes closest to

representing the extent of inundation within Poverty Bay. For Wainui the equivalent scenario is of an Outer Rise earthquake because this scenario inundates further on that piece of coast.

Due to the variability in earthquake slip, and the substantial uncertainty in fault parameters, it would be prudent to define evacuation zones in a way that incorporates a buffer around the selected scenarios.

8.4 Scenario Summary Table

The numerical simulation results were interpreted to provide an estimate of the tsunami intensity on the Papadopoulos and Imamura (2001) Tsunami Intensity scale (PI Scale, Table 8.4-1). The process of assigning a tsunami intensity is a subjective one, based on the report authors' considered opinion, and the table is intended as a guide to the relative severity of the scenario events rather than an indication of specific impacts.

The tsunami intensity scale proposed by Papadopoulos and Imamura incorporates twelve divisions (PI scale 1~12), consistent with the twelve-grade seismic intensity scales established and extensively used in Europe and North America over the last 100 years. The new scale is arranged according to (a) the effects on humans, (b) the effects on objects, including vessels of variable size, and on nature, and (c) damage to buildings.

1 - Not felt
- Not felt even under the most favourable circumstances.
- No effect.
- No damage.

2 - Scarcely felt
- Felt by few people on board small vessels. Not observed on the coast.
- No effect.
- No damage.

3 - Weak
- Felt by most people onboard small vessels. Observed by few people on the coast.
- No effect.
- No damage.

4 - Largely observed
- Felt by all onboard small vessels and by few people onboard large vessels. Observed by most people on the coast.
- Few small vessels move slightly onshore.
- No damage.

5 - Strong
- Felt by all onboard large vessels and observed by all on the coast. Few people are frightened and run to higher ground.
- Many small vessels move strongly onshore, few of them crash each other or overturn. Traces of sand layer are left behind on ground with favourable conditions. Limited flooding of cultivated land.
- Limited flooding of outdoors facilities (e.g. gardens) of near-shore structures.

6 - Slightly damaging

- Many people are frightened and run to higher ground.
- Most small vessels move violently onshore, or crash strongly into each other, or overturn.
- Damage and flooding in a few wooden structures. Most masonry buildings withstand.

7 - Damaging

- Most people are frightened and try to run to higher ground.
- Many small vessels damaged. Few large vessels oscillate violently. Objects of variable size and stability overturn and drift. Sand layer and accumulations of pebbles are left behind. Few aquaculture rafts washed away.
- Many wooden structures damaged, few are demolished or washed away. Damage of grade 1 and flooding in a few masonry buildings.

8 - Heavily damaging

- All people escape to higher ground, a few are washed away.
- Most of the small vessels are damaged, many are washed away. Few large vessels are moved ashore or crash into each other. Big objects are drifted away. Erosion and littering in the beach. Extensive flooding. Slight damage in tsunami control forest, stop drifts. Many aquaculture rafts washed away, few partially damaged.
- Most wooden structures are washed away or demolished. Damage of grade 2 in a few masonry buildings. Most RC buildings sustain damage, in a few damage of grade 1 and flooding is observed.

9 - Destructive

- Many people are washed away.
- Most small vessels are destroyed or washed away. Many large vessels are moved violently ashore, few are destructed. Extensive erosion and littering of the beach. Local ground subsidence. Partial destruction in tsunami control forest, stop drifts. Most aquaculture rafts washed away, many partially damaged.
- Damage of grade 3 in many masonry buildings, few RC buildings suffer from damage grade 2.

10 - Very destructive

- General panic. Most people are washed away.
- Most large vessels are moved violently ashore, many are destroyed or collide with buildings. Small boulders from the sea bottom are moved inland. Cars overturned and drifted. Oil spill, fires start. Extensive ground subsidence.
- Damage of grade 4 in many masonry buildings, few RC buildings suffer from damage grade 3. Artificial embankments collapse, port water breaks damaged.

11 - Devastating

- Lifelines interrupted. Extensive fires. Water backwash drifts cars and other objects in the sea. Big boulders from the sea bottom are moved inland.
- Damage of grade 5 in many masonry buildings. Few RC buildings suffer from damage grade 4, many suffer from damage grade 3.

12 - Completely devastating

- Practically all masonry buildings demolished. Most RC buildings suffer from at least damage grade 3.

Table 8.4-1 Estimated tsunami intensity of the studied scenario events according to the Papadopoulos and Imamura tsunami intensity scale (2001). Where the intensity varied spatially within a location the highest intensity estimate was used. The tsunami intensity in unoccupied areas is assigned as if they were developed. For each source earthquake the recurrence interval in years is given underneath in brackets, this figure is not adjusted to take into account the phase of the tide.

Source Scenario	Return Time	Gisborne	Muriwai	Wainui
M_W 9.1 in Peru (650)	Representative of 100 year distant source tsunami inundation	4	6	4
M_W 9.1 in Peru (HT) (650)		4-5	6	4-5
M_W 9.4 in Peru (3500)	Representative of 500 year distant source tsunami inundation	6	7	5
M_W 9.4 in Peru (HT) (3500)		6-7	8	6
Ariel Bank Fault (630)	Contribute to 100-500 year local source tsunami inundation	2-3	4	2-3
Gable End Fault (760)		2-3	3	3
Lachlan Fault (930)		3	4	2-3
Lachlan w/Deep Rup. (>930)		5	6	4
Lachlan w/Deep Rup. (HT) (>930)		6	7	5
Gisborne Segment M_W (>123)		4-5	6	3
GPS Coupling M_W (>400)		3	5	4
Whole Margin M_W 8.8 (>400)	May contribute to 500-2500 year local source tsunami inundation	6	7	5
Whole Margin M_W 9.0 (>800)		9	9	8
Whole Margin M_W 9.0 (HT) (>800)		9	10	8
Outer Rise M_W 8.0 (>1300)		3	5	8

In Table 8.4-1, the damages are classified into three categories, indicated by different colours: pink represents PI scale 9-10 (destructive), orange represents PI scale 5-8 (damaging) and pale green represents PI scale 1-4 (undamaging).

9.0 DISCUSSION

In this section we discuss various issues that are raised by the results presented in this report, and some of the limitations of the current work.

- Sand dunes

The coastal sand dunes play an important role in protecting inland areas of Poverty Bay from tsunami. Typically a sand dune will provide protection against incoming waves of up to about half the height of the dune. In region B (section 7) the 5.0 - 6.0m sand dunes are effective in preventing direct tsunami inundation in all but the worst case scenario. However, there is also a disadvantage to the presence of sand-dunes because, once the tsunami is capable of overtopping them, then huge volumes of water will be left behind the sand dunes after the tsunamis recede. Consequently, a flooding hazard may exist for much longer duration than the tsunami attack, and may result in salt water contamination of the fresh water environment.

Locations where the dunes are lower are more susceptible to inundation. Gaps in the dunes such as at the Grey Street road-end represent weak-points that may allow greater inundation than would otherwise take place. Protecting and maintaining the sand dunes is an effective means to mitigate the risk from tsunami.

- Erosion

In the present study, no erosion is considered. Therefore, no morphological changes to beaches and sand dunes that may occur due to strong current during overtopping are included in the modelling. Small gaps in sand dunes may become enlarged as fast flowing water passes through them, and the dunes can also be eroded during overtopping which leads to more severe inundation.

- Rivers and Bridges

Several scenarios show noticeable flooding of the rivers in Poverty Bay. The banks of rivers may present a tsunami hazard much further from the coast than the effects of overland inundation.

The LIDAR data used to define the topographic modelling grids may possibly include the elevation of bridge decks in some instances. Since tsunami waves may in practise flow under the bridge, our model may under-represent the true extent of up-river flooding in these cases.

- Effects on the Port

Port areas are particularly vulnerable to tsunami since they are low-lying and at the coast. Evidence for this comes from the 1960 tsunami which caused significant disruption to the Gisborne port, while not causing significant overland inundation. Just beside the wharf there is a cliff along Kaiti Beach Road (Titirangi Domain) where much higher tsunami runup heights are expected, and this causes a strong surge to traverse the wharf from the southeast to the northwest. Tsunami may displace materials that are sitting in ports, such as logs, and these can augment the destructive effect of the tsunami.

The return flow from Waikanae Creek and the Turanganui River also generates a strong current that flows out through the port, and could bring debris from land that may be deposited inside the port basin if the channel is not wide enough.

In most scenarios, the breakwaters were not effective enough to fully protect the port facility from the wave attacks.

- Roughness

In our model, surface roughness is represented using the Manning's n coefficient. This represents a significant approximation to the real effects of buildings and vegetation that impede the tsunami flow. Future work may attempt to use non-ground striking LIDAR data to explicitly represent obstacles to the flow.

- Non-uniform slip

Most of the scenarios used in this report assume earthquake ruptures with uniform slip (i.e. uniform amount of dislocation on the fault plane segments). Some are based on GPS coupling models which allow for smooth variations in slip. In actual ruptures, the slip on the fault plane varies in dislocation in complicated ways on a variety of spatial scales. The pattern of slip distribution cannot currently be predicted with any confidence. The pattern of slip distribution can affect the resulting tsunami (Geist, 1998). Our assumed uniform slip distribution may represent an approximate 'average' event compared to real earthquakes of the same magnitude which may have larger slip in some areas and lesser slip in others.

- Bay Oscillations

Modelling results indicate that oscillations of water in the bay will also put severe and long duration impacts on the surrounding areas in some scenarios. Poverty Bay is a partly enclosed water environment which inherently has its natural periods of oscillation. If the wave period of incoming tsunami is close to this natural period of bay oscillation, a phenomenon called resonance is going to occur and thus much stronger oscillations may follow the leading tsunami wave, and such oscillations may last several hours before settling down.

Poverty Bay has oscillations with a natural period of about 70 minutes. Tsunami from distant sources and those from local sources with relatively wide rupture areas (e.g., Lachlan Fault with deeper plate rupture) tend to exhibit periods close to or around one hour. This type of tsunami is more effective at exciting the bay oscillations, and therefore creates more severe flooding in the surrounding areas. These may last for several hours.

10.0 CONCLUSIONS

In this report we have developed several possible scenarios for tsunami events that could affect Poverty Bay and Wainui. For each scenario a model of the tsunami initiation at the source earthquake has been developed, the propagation from the source to Poverty Bay has been modelled, and the subsequent inundation, has been estimated.

The tsunami that can affect Poverty Bay can be divided into two groups: those that originate near the east coast of the North Island and are referred to as local source tsunami, and those that originate from other parts of the Pacific and are referred to here as distant source tsunami.

Distant source tsunami that cause damage in Gisborne are most likely to originate on the far side (i.e. east coast) of the Pacific. In particular, the west coast of South America has been the source region for three significant tsunami affecting Poverty Bay in the past 150 years.

The west coast of Central America is also well-oriented to produce tsunami whose waves propagate towards the southwest Pacific; but the past few centuries have not seen earthquakes occurring there that are large enough to be a significant hazard to Poverty Bay.

For the distant-source scenarios studied in this report we have chosen to model tsunami produced by earthquakes on the coast of Peru. The magnitudes of these scenario events have been chosen so that the extent of inundation in Poverty Bay is approximately representative of the inundation that is on average likely to occur due to distant-source tsunami every 100 and 500 years respectively. The impact on Poverty Bay of the modelled 100 year event is quite similar to that of the 1960 Chile tsunami (the worst distant source event of the past century), which provides an approximate validation of our methods.

In Gisborne the distant source 100 year inundation is confined mostly to the fringes of the port area and the Turanganui river mouth, while the 500 year distant source inundation is estimated to occur more widely in the coastal suburbs, the port areas, and on low-lying areas close to rivers. Muriwai, on the southwest of Poverty Bay, is estimated to be particularly affected by inundation in such an event.

There are many possible local sources of tsunami that could affect the Poverty Bay region. Some of these sources are earthquakes that rupture the interface between the Australian and Pacific continental plates, while others are earthquakes that rupture faults that lie within the overlying Australian plate or the subducting Pacific plate. Earthquakes that rupture both the plate interface and simultaneously faults within the crust of the Australian plate are also a possibility. Tsunami may also be caused by submarine landslides that occur near the edge of the continental shelf, but these are not studied in this report.

We have modelled a selection of these earthquake scenarios which is intended to provide a representative sample of the different types of events that could take place. For each scenario we estimated the vertical seabed deformation, which is the primary source of the tsunami waves. Using the well-tested COMCOT program, we have modelled the propagation of these waves to the coast and the subsequent inundation of the land in Poverty Bay and Wainui.

The Muriwai area was inundated in several of the scenarios. The low, flat landscape and the low height of the dunes at the coast provide little resistance to approaching tsunami. Near Gisborne city the coastal dune is higher, and this provides a substantial degree of protection. Inundation is most likely to occur around the Turanganui river mouth, the port area, and near gaps in the sand dune. Only in the most severe scenario is the coastal sand dune widely overtopped. In Wainui the height of the steep beach face appears to provide protection in many of the scenarios, although the lower-lying areas surrounding the creeks were often inundated. Interestingly the worst scenario for Wainui is an earthquake in the outer rise of the Pacific plate, whereas within Poverty Bay the most severe scenario was one of a large earthquake on the plate interface.

Because of the wide variety of possible sources, and our limited understanding of them, it is very difficult to systematically estimate the inundation at specific return times in the manner that was done for the distant sources.

At return times of up to 100 years the local source hazard appears likely to be dominated by tsunami originating from earthquakes similar to the two that occurred in 1947, and one that probably occurred in 1880. It has recently been established that both 1947 earthquakes occurred close to the locations of subducting seamounts. An unusual feature of these earthquakes is that they caused relatively little shaking, and this represents a problem for risk mitigation as it is likely that few people will self evacuate in similar future events. We have not modelled events of this type for this report, as the impacts of the 1947 tsunami events are well documented.

At return times between 100 and 500 years the local source tsunami hazard appears likely to be contributed to by earthquakes on faults in the crust of the Australian plate, such as the Lachlan and Ariel Bank faults, and by earthquakes on the plate interface with magnitudes of up to about M_W 8. In some instances rupture on crustal faults and the plate interface may occur simultaneously. It should be noted that many of these sources have individual recurrence intervals (the average time between events) that are greater than 500 years, but the cumulative effect of several such sources will determine which areas can expect on average to be inundated every 100-500 years.

At return times between 500 and 2500 years there is a great deal of uncertainty regarding the main sources of tsunami hazard. Ruptures of the plate interface along the whole Hikurangi margin are one possibility, but currently no paleotsunami or paleoseismology evidence has been identified for such events. Plate interface earthquakes confined to the Hawke's Bay and Raukumara Peninsula region, with magnitudes up to about M_W 8.5, might have similar impacts. Tsunami caused by earthquakes on the Outer Rise (the part of the Pacific plate that is being bent prior to subduction) are a distinct possibility, and our modelling suggests that Wainui is particularly vulnerable to these. Landslide-caused tsunami may become significant contributors to the tsunami hazard on this time scale.

11.0 REFERENCES

Ando, M., 1975. Source mechanisms and tectonic significance of historical earthquakes along the Nankai Trough, Japan. Tectonophysics, 27: 119-140.

Bell, R.E., Sutherland, R., Barker, D.H., Henrys, S.A., Bannister, S.C., (2008), *Eos Trans. AGU,* 89(53), Fall Meet. Suppl., Abstract T23A-1995

Cho, Y.-S. (1995). Numerical simulation of tsunami and runup. PhD thesis, Cornell University, 1995.

Collot, J.-Y., Lewis, K., Lamarche, G., and Lallemand, S. (2001). The giant Ruatoria debris avalanche on the northern Hikurangi margin, New Zealand; results of oblique seamount subduction, Journal of Geophysical Research, 106, 19.

Geist, E.L. (1998), Local tsunamis and earthquake source parameters, Advan. Geophys. 39, 117–209.

Goldfinger, C., Morey-Ross, A., Erhardt, M., Nelson, C.H. and Pastor, J., 2006. Cascadia great earthquake recurrence: rupture lengths, correlations and constrained OxCal analysis of event ages. USGS Tsunami Sources Workshop, April 21-22, 2006.

Imamura, F., Yalciner, A.C., and Ozyurt, G. (2006). Tsunami modelling manual, 58 p. http://ioc3.unesco.org/ptws/21/documents/TsuModelMan-v3-ImamuraYalcinerOzyurt_apr06.pdf.

Liu, P.L.-F., Cho, Y.-S., Yoon, S.B. and Seo, S.N. (1994). Numerical simulations of the 1960 Chilean tsunami propagation and inundation at Hilo, Hawaii. In Recent Development in Tsunami Research, pp99-115. Kluwer Academic Publishers, 1994.

Liu, P.L.-F., Cho, Y.-S. and Fujima, K. (1994). Numerical solutions of three-dimensional run-up on a circular island, Proc. Of Int. Sym.: Waves – Physical and Numerical Modelling, pp. 1031-1040, Canada.

Liu, P.L.F., Cho, Y.-S., Briggs, M.J., Synolakis, C.E. and Kanoglu, U. (1995). Run-up of solitary waves on circular island. J. Fluid Mech., 302:259-285, 1995.

Liu, P.L.-F., Wang, X. and Salisbury, A. J. (2009). Tsunami hazard and early warning system in South China Sea. Journal of Asian Earth Science. Accepted on Dec 26, 2008, to be published in 2009.

Liu, P.L.-F., Woo, S.-B. and Cho, Y.-S. (1998). Computer programs for tsunami propagation and inundation. Technical Report, Cornell University, 1998.

Liu, P.L.-F. and Wang, X. (2008). Tsunami source region parameter identification and tsunami forecasting. Journal of Earthquake and Tsunami. Vol.2, No.2 (2008) pp.87-106.

Murashima, Y., Takeuchi, H., Imamura, F., Koshimura, S., Fujiwara, K., and Suzuki, T.(2008). The International Archives of the Photogrammetry, remote Sensing and Spatial Information Sciences. Vol. XXXVII. Part B8. pp.223-228.

Power, W.L.; Reyners, M.E.; Wallace, L.M. (2008). Tsunami hazard posed by earthquakes on the Hikurangi subduction zone interface.:. *GNS Science consultancy report 2008/40.* 58 p.

Reyners, M., 1998. Plate coupling and the hazard of large subduction thrust earthquakes at the Hikurangi subduction zone, New Zealand. New Zealand Journal of Geology and Geophysics, 41(4): 343-354.

Van der Sande, C.J., de Jong, S.M., de Roo, A.P.J. (2003). A segmentation and classification approach of IKONOS-2 imagery for land cover mapping to assist flood risk and flood damage assessment. International Journal of Applied Earth Observation and Geoinformation. Vol.4. pp. 217-229

Wallace, L.M. and Beavan, J., 2006. A large slow slip event on the central Hikurangi subduction interface beneath the Manawatu region, North Island, New Zealand. Geophys. Res. Lett., 33, L11301, doi:10.1029/2006GL026009.

Wallace, L.M., Beavan, J., McCaffrey, R. and Darby, D., 2004. Subduction zone coupling and tectonic block rotations in the North Island, New Zealand. J. Geophys. Res, 109(B12406): doi:10.1029/2004JB003241.

Wang, X. and Liu, P.L.-F. (2005). A numerical investigation of Boumerdes-Zemmouri (Algeria) earthquake and tsunami. Computer Modeling in Engineering and Science, Vol.10, No.2, pp.171-184.

Wang, X. and Liu, P. L.-F. (2006). An analysis of 2004 Sumatra earthquake fault plane mechanisms and Indian Ocean tsunami. Journal of Hydraulic Research, Vol. 44, No.2 (2006), pp.147-154.

Wang, X. and Liu, P. L.-F. (2007). Numerical simulation of the 2004 Indian Ocean tsunami – Coastal Effects. Journal of Earthquake and Tsunami. Vol.1, No.3 (2007). pp273-297.

Wang, X., Orfila, A. and Liu, P.L.-F. (2008). Numerical simulations of tsunami runup onto a three-dimensional beach with shallow water equations. ACOE. vol.10, pp.249-253, 2008. World Scientific Publishing Co.

Wang, X. (2008). Numerical Modelling of surface and internal waves over shallow and intermediate water. PhD thesis, Cornell University 2008.

Wijetunge, J. J., Wang, X. and Liu, P. L.-F. (2008). Indian ocean tsunami on 26 December 2004: numerical modelling of inundation in three cities on the south coast of Sri Lanka. Journal of Earthquake and Tsunami. Vol.2, No.2 (2008) 133-155.

www.gns.cri.nz

Principal Location

1 Fairway Drive
Avalon
PO Box 30368
Lower Hutt
New Zealand
T +64-4-570 1444
F +64-4-570 4600

Other Locations

Dunedin Research Centre
764 Cumberland Street
Private Bag 1930
Dunedin
New Zealand
T +64-3-477 4050
F +64-3-477 5232

Wairakei Research Centre
114 Karetoto Road
Wairakei
Private Bag 2000, Taupo
New Zealand
T +64-7-374 8211
F +64-7-374 8199

National Isotope Centre
30 Gracefield Road
PO Box 31312
Lower Hutt
New Zealand
T +64-4-570 1444
F +64-4-570 4657